Review article

# Advances in catalysts for direct syngas conversion to light olefins: A review of mechanistic and performance insights

Elham Mahmoudi [a], Ali Sayyah [b], Samira Farhoudi [a], Zahra Bahranifard [b], Gamze Behmenyar [c], Abdullah Z. Turan [c], Nagihan Delibas [d], Aligholi Niaei [a,d,*]

[a] Department of Chemical and Petroleum Engineering, University of Tabriz, Tabriz, Iran
[b] Department of Chemical Engineering, Virginia Polytechnic Institute and State University, Blacksburg, VA 24061, United States
[c] TUBITAK Marmara Research Center, Energy Institute, Kocaeli, Turkey
[d] Department of Physics, Faculty of Science, University of Sakarya, Sakarya, Turkey

ABSTRACT

Light olefins are critical chemical materials with high global demand. The syngas-to-olefins (STO) process offers a promising pathway for light olefin production due to the versatility of syngas production technologies from various energy sources. However, achieving high carbon monoxide (CO) conversion and selectivity for olefins remains a challenge in catalytic development. This review categorizes STO catalysts into conventional Fischer-Tropsch catalysts, including unsupported and supported metal-based catalysts (with supports such as carbon, graphene, graphene oxide, zeolites, and metal oxides), as well as bifunctional, hybrid, and emerging core@shell structured catalysts. Another type of catalyst is core@shell structure catalyst, which is a developing method widely used for FT reactions. The performance of these catalysts is influenced by their materials, chemical compositions, operating conditions, and synthesis techniques. Unsupported catalysts, especially Fe-based and Co-based, exhibit high CO conversion but face issues like rapid deactivation and complex processing requirements. Supported catalysts enhance surface area, metal dispersion, and stability, with promoters such as Na, Mg, K, Mn, Zn, V, Zr, and Cu oxides improving catalytic activity through better CO adsorption and bond modulation. Zeolites, due to their acidic properties, significantly impact reactant adsorption and activation. Catalyst preparation methods, including impregnation, co-precipitation, sol-gel, and hydrothermal synthesis, alongside post-synthesis treatments like calcination and reduction, critically affect catalyst performance. This review provides a comprehensive overview of the light olefin production from syngas, detailing the roles of various catalysts and the impact of material types, operating conditions, and synthesis techniques on catalyst activity, and selectivity. The insights aim to guide future research and development towards more efficient and sustainable light olefin production processes.

## 1. Introduction

Olefin refers to an unsaturated chemical molecule characterized by the presence of at least one carbon-carbon double bond. Among the simplest olefins are ethylene, propylene, and butylene, collectively known as light olefins [1,2]. The production of light olefins ($C_2$-$C_4$=) employs various methodologies, which have become customary in diverse chemical and petrochemical industries [3,4]. The utilization of feedstocks obtained through the cracking of raw materials like natural gas and crude oil is particularly prominent, making it a favored technique within the petrochemical sector [5,6]. These carbon-based building blocks play a pivotal role in generating a variety of materials, including chemical intermediates and industrial solvents. Notably, the primary products of naphtha steam cracking are ethylene and propylene [7]. This process inherently yields propylene as a byproduct, and fine-tuning the cracking process intensity offers the means to modify the propylene/ethylene ratio [6,8].

In the contemporary landscape, there is a global surge in the demand for light olefins. The increasing global demand for light olefins, coupled with the finite nature of traditional oil-based feedstocks and the associated environmental impact, underscores the importance of exploring alternative production methods such as syngas conversion. Light olefins

---

are crucial feedstocks and platform molecules for the chemical industry. The annual production of the primary olefins, ethylene and propylene, is $1.5 \times 10^8$ and $8 \times 10^7$ tons, respectively [9,10]. The market potential of light olefin production via syngas conversion is significant, especially given the rising demand for transportation fuels, estimated at 40–45 million barrels per day (bbl./day) which accounted for 24 % of global $CO_2$ emissions in 2016 according to the International Energy Agency (IEA) [11–13]. These factors highlight the need for sustainable and efficient production technologies, positioning syngas conversion as a promising solution to meet both economic and environmental objectives in the global chemical industry. The market possibility for light olefin production via syngas conversion is driven by several key factors: the abundant availability of feedstocks like natural gas, coal, and biomass; advances in catalytic processes enhancing efficiency and selectivity; and growing environmental regulations promoting sustainable and low-carbon technologies. Furthermore, advancements in bi-functional catalysts have improved the efficiency and selectivity of the syngas-to-olefins process, with current technologies achieving olefin yields of up to 50 %, compared to yields of 30–35 % a decade ago [14, 15]. These technological improvements, coupled with favorable economic and environmental policies, are expected to sustain robust growth in syngas-based light olefin production in the future.

However, a significant challenge arises due to the finite nature of oil sources, which are pivotal as feedstock for light olefin production, particularly for ethylene and propylene [1]. The utilization of oil sources, being non-renewable, results in one of the most energy-intensive processes for light olefin production and concurrently generates substantial carbon dioxide ($CO_2$) emissions [16]. In response to these challenges, researchers have grappled with intricate issues over the past decades. The key focal points have been the transformation of light olefin production methods and the primary feedstock [15,17]. Traditionally, synthesis gas, a mixture of hydrogen ($H_2$) and carbon monoxide (CO) gases, has been a cornerstone source for light olefin production. This versatile resource is conventionally derived from biomass, coal, natural gas, and oil [18]. Notably, biomass and coal have emerged as viable alternatives for sourcing synthesis gas. Coal presents an optimal choice for regions rich in coal deposits, while biomass garners attention as a renewable and economically viable option [17,19]. An established technique for converting syngas into linear hydrocarbons is the Fischer-Tropsch (FT) synthesis, characterized by the Anderson-Schulz-Flory (ASF) distribution principle [20]. The resultant product distribution in the FT process hinges upon factors such as the catalyst's intrinsic properties and operational parameters, including the $H_2$/CO ratio within the syngas, process temperature, and pressure settings [21,22]. It is imperative that the synthesis gas used for diverse hydrocarbon production be of utmost purity, devoid of contaminants, with a particular emphasis on sulfur (S) compounds. These compounds, prevalent in coal and natural gas, are acknowledged catalyst inhibitors in FT synthesis [23].

There are different ways to produce light olefins from synthesis gas. During this syngas-to-olefins transformation process, the $H_2$/CO ratio, may need adjustment via the the water gas shift reaction (WGSR) (Eq. 1) [24].

$$CO + H_2O \leftrightarrow CO_2 + H_2 \tag{1}$$

After adjusting the $H_2$/CO ratio, methanol, lower alcohol, FT liquids, and dimethyl ether can be synthesized. Light olefins can be derived in the subsequent steps by using intermediate products from different processes like methanol-to-olefins (MTO), dehydration, cracking, and dimethyl ether to the olefin process. This process is known as the indirect light olefin production process [6,25,26]. Besides these indirect routes, another alternative syngas-to-olefin production method is direct Fischer-Tropsch-to-olefins (FTO). The direct conversion of synthesis gas to light olefin doesn't require adjustment of $H_2$/CO ratio. This process can be performed by modifying conventional FT catalysts, some of which have exhibited high selectivity toward light olefin (FTO) [9].

During FTO synthesis, multiple reactions, including paraffin and olefin formation, can proceed as follows (Eqs. 2 and 3) [27].

$$nCO + (2n + 1)H_2 \leftrightarrow C_nH_{(2n+2)} + nH_2O \tag{2}$$

$$nCO + 2nH_2 \leftrightarrow C_nH_{2n} + nH_2O \tag{3}$$
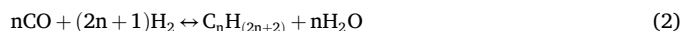
In recent decades, researchers have focused on the new generation of hybrid catalysts called bi-functional catalysts for the direct production of light olefins from synthesis gas, which have shown high selectivity. These catalysts typically contain a metal base with zeolite or metal supports that can increase the fraction of light olefins in the products [28].

This study aims to present an extensive overview of different bulk, supported, and bi-functional catalysts that have been synthesized by various methods and used for light olefin production from syngas under different operation conditions. For this purpose, different methods used for light olefin production were studied, and all factors influencing the behavior of the catalyst including material type, chemical composition, operating conditions and synthesis process have been assessed.

## 2. Light olefin production

Light olefins are a group of chemicals of high industrial significance, serving as intermediate raw materials in the synthesis of many products. Derivatives of light olefins are used in furniture, dyes, kitchen appliances, and other everyday items. Various technologies produce these components in different parts of the world, depending on their local energy sources. The predominant technology for light olefin production is naphtha steam cracking, which uses crude oil as feedstock [29]. However, alternative technologies also exist, primarily based on syngas production (Fig. 1) [6]. In this context, coal and biomass are the most important sources of raw materials for syngas production via gasification. Syngas-based light olefin technologies can be either direct or indirect production methods, while a more innovative approach is the direct production of olefins in a single step. One direct production method involves producing of olefins via Fischer-Tropsch (FT) process. Currently, there is no commercial application of this method, but there is growing interest in R&D activities aimed at developing suitable catalysts. Today, selecting the right production technology depends not only on the performance criteria, such as the selectriviy for $C_2$-$C_4$= plefins, but also on environmental consideration [30].

The production of light olefins through various technologies and using different types of industrial feedstocks, including heavy naphtha and synthesis gas from coal, biomass, and natural gas sources, is discussed in the following sections.

### 2.1. Steam cracking process

Steam cracking (SC) of hydrocarbons is a high-temperature, energy-intensive process that has been extensively used in petrochemical industries as the primary source of light olefins for the past century [31, 32]. Naphtha and ethane are the main feedstocks used for SC. This process has some notable disadvantages, including high $CO_2$ emissions and challenges in controlling the propylene-to-ethylene ratio [33,34]. In SC a mixture of hydrocarbons and steam is heated to the primary cracking temperature. Product formation in the reaction depends on factors such as the feed composition, the ratio of hydrocarbon to steam, reaction temperature, pressure, and furnace residence time, all of which require careful control. Generally, SC for light olefin production, with ethylene as the major product, operates at high temperatures, low pressure, and short residence times. Upon reaching the cracking temperature (around 850°C), the gas is rapidly quenched to halt the reaction in a transfer line exchanger. Free-radical chain reactions are widely accepted as the primary mechanisms for hydrocarbon thermal cracking [35–37]. Fig. 2 presents the mechanism of SC [38].

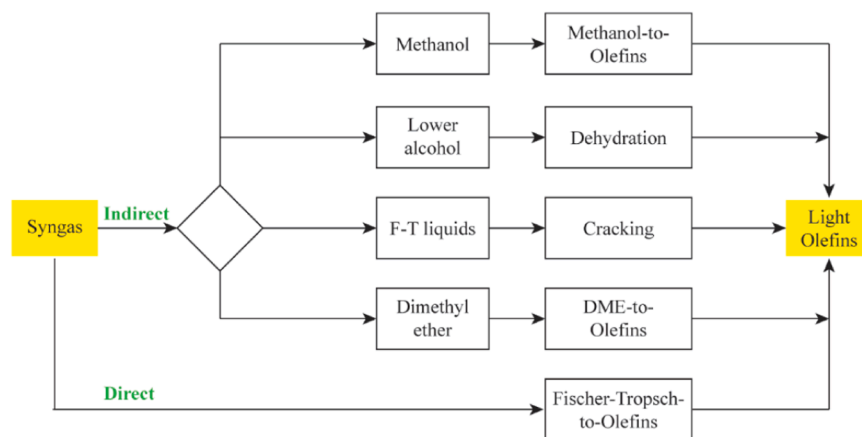The SC process comprises three sections, with the pyrolysis section

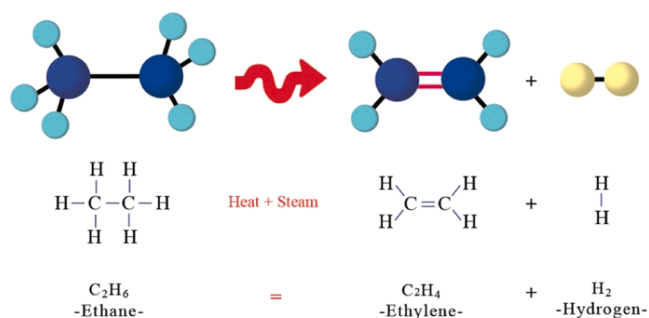**Fig. 1.** Routes for light olefin production from syngas [6].



**Fig. 2.** Steam cracking mechanism [38].

being the most critical. In this section, feedstock enters a series of heat exchangers in the convection section, where it is vaporized with superheated steam and cracked into smaller molecules without the use of catalysts. For feedstocks like naphtha or gas oil, the second section involves primary fractionation, where streams containing gasoline and fuel oil (rich in aromatics) are condensed and fractionated. The final section involves product separation, which utilizes distillation, refrigeration, and extraction processes [39]. As mentioned, achieving high yields of light olefins, hinges significantly on the reaction conditions and properties of the catalysts employed. Various types of catalysts, such as oxide, zeolite, zeotype-based, and carbon nanotube (CNT)-based catalysts, have been studied [40].

The use of $KVO_3$-impregnated $\alpha$-$Al_2O_3$ catalyst yielded approximately 34.5 % ethylene and 16.6 % propylene in a fixed bed reactor [41]. In a distinct approach, using molybdenum oxide ($MoO_2$) in a batch reactor resulted in ethylene and propylene yields of 29 % and 35 %, respectively [42]. In recent decades, catalysts such as MgO, $TiO_2$, $MnO_2$, $Mn_2O_3$, $ZrO_2$, $K_2O$, and $In_2O_3$ have shown notable efficacy in increasing the yields of light olefins [33]. Additionally, the use of $VO_x$/$SrO$-$\gamma Al_2O_3$ demonstrated an impressive 88 % selectivity for olefins [43].

Recently, zeolites have gained substantial traction in the oil and gas sectors, prominently as catalytic cracking catalysts [44,45]. Among them, ZSM-5 and HZSM-5 have demonstrated superior performance in catalytic cracking of hydrocarbons, yielding enhanced quantities of light olefins compared to other zeolite variants [46]. This exceptional performance can be attributed to their efficacious activation mechanisms and well-defined porous structures [47]. Activated carbon-based materials offer another promising avenue for catalytic cracking reactions, owing to their notable attributes such as high surface area and thermal stability at elevated temperatures. These qualities make them compelling candidates for catalytic applications [48,49].

## 2.2. Production of light olefin from syngas

### 2.2.1. Syngas production

Using steam cracking of naphtha for light olefin production poses environmental problems such as global warming (due to $CO_2$ emissions) and the depletion of fossil fuels. $H_2$, which can be produced through various chemical processes such as biomass gasification, and ethanol or methanol steam reforming, is considered a clean fuel for future use [50]. Fossil fuel reforming, mainly of natural gas, accounts for about 90 % of the total $H_2$ production [51]. Synthesis gas can be generated from any hydrocarbon feedstock, including natural gas, naphtha, residual oil, petroleum coke, and coal [52]. The conversion of fossil feedstocks to transportation fuels involves producing hydrocarbon mixtures where controlling the $H_2$/CO ratio is crucial. This often requires the addition of $H_2$ to the feedstock by hydrotreating and hydrocracking [51]. Steam reforming typically achieves an $H_2$/CO ratio of about 3, while partial oxidation results in an $H_2$/CO ratio of about 2 when producing synthesis gas from natural gas. For coal or biomass as the feedstock, gasification is the typical process. The required $H_2$/CO ratio for coal ranges from about 0.42–1, and for biomass, it ranges from about 0.62–1. Synthesis gas from coal sources contains sulfur species ($H_2S$ and COS), hydrogen chloride, ammonia, hydrogen cyanide, and volatile species of trace metals such as mercury, arsenic, and selenium, all of which require removal through purification processes [53].

There are different processes for light olefin production from syngas, such as through methanol, dimethyl ether, lower alcohol, which are then converted into light olefins. The most critical indirect routes studied in recent decades, with strong potential for commercialization, are the MTO and DMTO processes. Producing light olefins directly from synthesis gas using bifunctional catalysts is another promising approach (Fig. 3) [6].

### 2.2.2. Methanol-to-Olefins (MTO) process

The MTO reaction is pivotal for producing olefins from synthesis gas, first discovered in 1977 by researchers at Mobil using aluminosilicate zeolite as the catalyst. This process forms a crucial link between biomass, natural gas, coal, and petrochemical primary raw materials [54–56]. The first MTO unit, which utilized coal-derived synthesis gas, was constructed and began operation in China in 2010. This milestone has been regarded as a significant advancement in global light olefin production [57]. The success of the MTO process heavily depends on type of catalyst used, with acidic zeolite catalysts being essential for optimal performance. Without these catalysts, the chemical reactions in the MTO process would proceed too slowly to be economically viable [58].

In 1982, researchers at the Dalian Institute of Chemical Physics (DICP) initiated investigations into the MTO process, focusing initially on zeolite modification. They studied catalysts like ZSM-5, small-pore
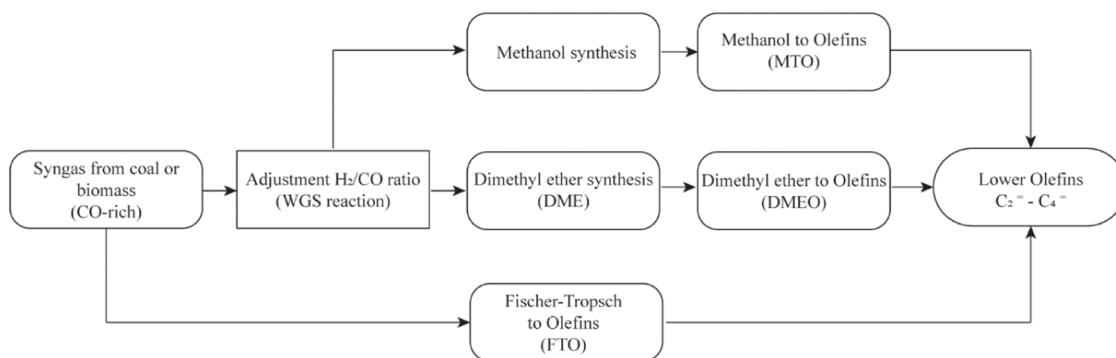
**Fig. 3.** Direct and indirect routes for light olefin production [6].

molecular sieves, and zeolites with optimized acid functions such as SAPOs. These studies revealed that these catalysts are optimal for the MTO process due to their shape selectivity, acidity, and topology. Subsequently, extensive research on these catalysts has been conducted by researchers worldwide [57,59,60]. The Si/Al ratio, synthesis method, and selected template influence the zeolite structure and physico-chemical properties. In recent years, H-SAPO-34 (CHA) and H-ZSM-5 (MFI) with 8–10 membered rings, have been identified as effective and stable catalysts for the MTO process [57,61]. The catalytic performance of MTO reactions has been studied using nano SAPO catalysts with different silicon percentages [62]. Catalyst deactivation during the process is a critical factor in catalyst design. A comparative study between isostructural H-SAPO-34 and H-chabazite in the MTO reaction showed that the deactivation rate depended on acid site density [63,64]. Recently, numerous studies have focused on enhancing the performance of widely used commercial catalysts. These include, developing theoretical models for olefin diffusion in HZSM-5 and HSAPO-34 zeolites during the MTO reaction [65], studying the effect of metal ion incorporation on the structure and acidity of SAPO-34 molecular sieves [66], investigating the impact of intracrystalline macropores on the deactivation behavior of ZSM-5 catalysts during MTO conversion [67], analyzing the regeneration kinetics of coke on industrial MTO catalyst [68], exploring of the influence of spatially distributed pore size and porosity on diffusional and reactive features in MTO catalyst particles [69], examining the impact of Zn addition in the cavities of the shell layer of SAPO-34 catalyst [70], and modelling the effect of coke formation on diffusion and adsorption in SAPO-34 using the dual-cycle mechanism and Maxwell-Stefan diffusion theory [71]. These studies represent recent and significant advancements in the field of MTO reaction research.

*2.2.3. Dimethyl ether to olefin (DMTO) process*

DMTO process is another important indirect route to light olefin production from syngas, offering several advantages over other methods, such as enhanced CO conversion and simplified process [72]. DMTO processes are more desirable than MTO processes due to their thermodynamic characteristics and great potential to give high olefin yield and selectivity. Smilar to the MTO process, the DMTO process is based on heterogeneous catalysts, which play a crucial role in its efficiency and effectiveness [73]. Recently, there has been research focused on the production of lower olefins from dimethyl ether. Investigation of effects of the particle size of a suspended zeolite catalyst on its characteristics and catalytic properties in the conversion of dimethyl ether to light olefin [73], designing a nano dispersed catalyst suspensions that are active and stable in converting DME into light olefins from MFI commercial zeolite samples [74], studying the effect of operation temperature over La-Zr supported ZSM-5 and alumina ($Al_2O_3$) catalysts [75], analyzing the impact of structure and Bronsted acidity of a zeolitic material like ZSM-5 and Y zeolites on DMTO catalysts activity [76], studying the effect of additives like $TiO_2$ and S for HZSM-5 catalyst [77],

evaluation of the activity of hierarchical mordenite (MOR) zeolites [78, 79], investigation of the conversion of DMTO over Ca-ZSM-5, La-ZSM-5 and Ca-La-ZSM-5 [80], determination of kinetic models and deactivation equations for DMTO process over HZSM-5 zeolite [81,82], studying the deposition of coke in a HZSM-5 zeolite-based catalyst during the DME conversion and its regeneration through combustion of coke [83], the evolution and distribution of products during the reaction of DMTO process over SAPO-34 as catalyst [84], investigation of the reaction of DMTO over HZSM-5/$Al_2O_3$ catalysts modified by Zr and Mg and stabilized by hydrothermal treatment [85], systematically study of the influences of template composition and crystallization time of SAPO-34 catalysts that are used in DMTO process [86] are some of the most important recent studies for DMTO process.

**3. Direct light olefin synthesis catalysts**

Light olefin production through the MTO and DMTO processes has been studied for years, and today, the MTO process has been commercialized and is recognized as the main route for light olefin production. However, this commercial process has drawbacks, such as its multi-step nature, which can lead to lower process efficiency. Reactor selection, catalyst structure, and temperature control can cause major limitations in industrial settings, and they should be carefully considered in the process design of light olefin production from syngas [17,87,88]. The FTO synthesis for direct light olefin production from syngas, governed by the Anderson-Schulz-Flory (ASF) rule, achieves a maximum selectivity of approximately 58 % for light olefins and 25 % for methane. Despite, its potential, this approach is not widely favored in industrial applications [89,90]. This strategy involves combining FT-active catalysts with the acid function of zeolites that are active in the MTO process, creating bifunctional catalysts that can operate in a single reactor or multiple reactors [91]. This approach offers several advantages, such as higher efficiency in energy and cost. However, it also has disadvantages, notably lower selectivity towards light olefins compared to indirect routes [18].

In the direct light olefin production via FTO, two types of catalysts are commonly employed: conventional FT catalysts and bifunctional catalysts. Conventional FT catalysts typically consist of transition metals such as iron (Fe), cobalt (Co), or nickel (Ni), often supported on materials like silica ($SiO_2$) or alumina ($Al_2O_3$). These catalysts may also include promoters or modifiers to enhance selectivity towards light olefins. In contrast, bifunctional catalysts consist of two distinct functional components: a metal component (such as Cu, Fe, or Co) and an acidic component (usually a zeolite or other solid acid). These different catalysts lead to distinct mechanisms and reaction pathways for direct light olefin production. Conventional FT catalysts modify traditional FT synthesis routes to favor light olefins, while bifunctional catalysts use a two-step process involving intermediate formation followed by conversion to light olefins through acid-catalyzed reactions [92,93].

### 3.1. Conventional FT catalysts

conventional FT catalysts are generally classified into supported and unsupported types, each with distinct characteristics and applications. Unsupported catalysts are particularly effective in achieving high selectivities towards lower olefins, but they often exhibit low mechanical stability due to significant carbon deposition [17]. The performance of supported and unsupported Fe and Co catalysts has been investigated by Schneider [94,95].

The catalytic properties of unsupported catalyst, such as activity and selectivity in the FT process, are primarily determined by the main metal element. Metals from Groups IV to VI, like Zr, Ti, Mo, etc., are known for promoting dissociative CO adsorption, a crucial step necessary for FT synthesis to proceed. However, these metals tend to form very stable oxides, which cannot be reduced under FT conditions, preventing the generation of FT active sites. while, Group XI-XII metals (Cu, Zn), as well as precious metals like Pt and Pd can dissociate CO, they generally exhibit poor activity for FT-to-olefins conversion. On the other hand, metals such as Fe, Co, Ni, Ru, and Os have been reported to show significant activity for FT reactions. Though not that widespread, some studies have reported sufficient FT-to-olefins activity using Re and Rh metals. Among all these metals mentioned, Fe- and Co-based catalysts are the most commonly used catalysts in the FTO process. Utilizing carbide forms of these metals for catalytic activity is the conventional way to produce lower olefins via FT [94,96].

The widely accepted mechanism for unsupported FTO catalysts involves a series of surface reactions optimized to maximize the formation of light olefins (ethylene, propylene, butenes) from syngas (i.e., the carbide mechanism). Initially, CO and $H_2$ molecules adsorb onto the catalyst surface, where transition metals provide active sites for their dissociation. The CO dissociates into carbon and oxygen atoms, while hydrogen atoms facilitate the formation of surface-bound $CH_3$ species (Fig. 4) [97,98]. These species then react with additional CO and $H_2$ to propagate hydrocarbon chain growth, primarily forming surface carbides ($C_xH_y$). The conditions are optimized to favor short-chain hydrocarbons through repeated insertion of $CH_2$ units. Chain termination occurs via beta-hydride elimination, leading to the formation of double bonds and the release of light olefins, which desorb from the catalyst surface. As mentioned before, the selectivity towards light olefins is influenced by several factors, including the catalyst composition, the addition of promoters or modifiers, and the reaction conditions such as temperature and pressure. Higher temperatures and lower pressures generally enhance olefin selectivity by favoring chain termination and desorption of shorter hydrocarbons. Additionally, the surface structure and morphology of the catalyst play a crucial role in determining the product distribution. By precisely controlling these parameters, the FTO process can be tailored to efficiently convert syngas into valuable light olefins [99–101].

### 3.1.1. Effect of promoters on the performance of Fe/Co-based catalysts

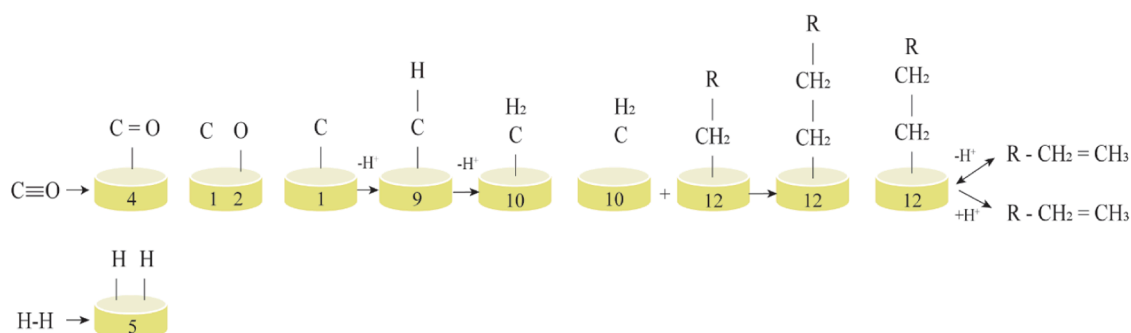Iron (Fe) nanoparticles are useful in the manufacture of olefins due to their ability to promote the formaion of olefins and oxygenates over paraffin. They are also favored since it is quite simple to prepare active Fe phases for subsequent applications [103]. Additionally, Fe-catalyzed light olefin synthesis can be improved by adjusting process variables (such as temperature) [94,104,105]. However, these catalysts are deactivated rapidly, and tend to generate more undesirable products like methane, which is a drawback for commercial applications [102]. Another notable disadvantage of these catalysts is the deprivation of their mechanical stability, like degradation by high temperatures or blocking by some unwanted chemicals [17].

On the other hand, Co-based catalysts are known for their activity and selectivity towards linear long-chain hydrocarbons and are more resistant to deactivation by the produced water ($H_2O$) during the reaction. However, they need a complex matrix of downstream unit operations, and they are costly, which is undesirable in respect of the process economy [106]. A promising way to enhance the FTO catalytic activity is to add some promoters such as Na, Mg, K, Mn, Zn, V, Zr, and Cu oxides to Fe and Co catalysts (Fig. 5) [107–113].

- **Alkaline Metals as promoters**

  Sodium (Na) and potassium (K) can become primary catalyst promoters since they raise CO adsorption and attenuate the CO bond due to their electronic modulation [115]. The studies showed that the presence of alkali metal promoters in the CoMn catalysts benefited the formation and stabilization of the $Co_2C$ phase, decreasing methane selectivity while increasing light olefin selectivity [116]. Comparing different catalysts containing K and Na alkali metals as electronic promoters, revealed that CO conversion
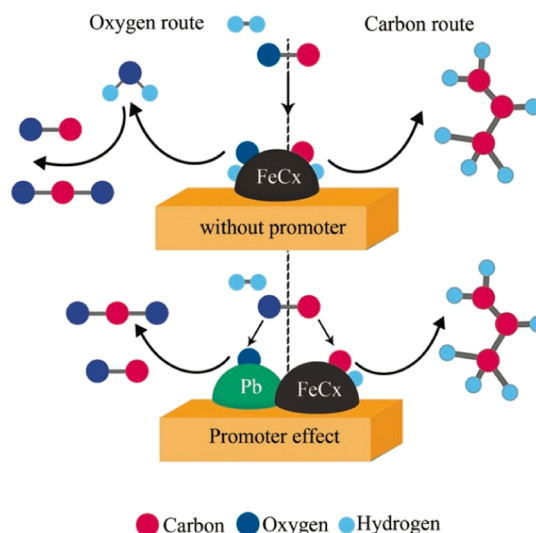
**Fig. 5.** Influence of promotion with soldering atoms on FT synthesis [114].

**Fig. 4.** The carbide mechanism for FT synthesis [102].

reaches 94.5 % by using FeMn, but extra Mn leads to a dip in CO conversion. This amount was further increased by adding promoters (96.2 % for FeMnNa and 95.0 % for FeMnK). The enhancement of the performance of catalysts was indeed obvious by not only maximizing CO conversion but also creating some peaks in both selectivities of light olefins and O/P ratio when K-promoted Fe catalysts (2.8 mol% K/Fe ratios) were used. Besides, the only disadvantage of the K-Fe catalyst is the high amount of methane (12.55 %) compared with other types of catalysts. The reason is that K promotes the chemisorption of adsorbed hydrogen (H*) on the catalyst surface due to its strong surface basicity and electron-donating ability. Enhanced H* chemisorption might lead to a high concentration of hydrogen atoms on the catalyst surface. The adsorbed hydrogen atoms can readily react with olefins, leading to the saturation of double bonds and the formation of methane, a fully saturated hydrocarbon [94, 117,118].

Activation conditions such as calcination temperature are also important factors affecting catalytic performance. In a study, an FeZn mixed metal oxide catalyst with a Na promoter was synthesized by co-precipitation and wet impregnation methods at five calcination temperatures (350, 400, 500, 600, and 700°C). The catalyst synthesized at a calcination temperature of 400°C exhibited the best CO conversion performance over 50 h (1.3–1.8 times higher than others). This result can be attributed to several factors, including better development of a crystalline structure that promotes the formation of active Fe carbide ($Fe_5C_2$) species and improved dispersion of Na species on the surface. The catalyst also exhibited a higher hydrocarbon yield compared to others (49.7 % hydrocarbon yield), with 32.9 % selectivity for olefins, 18.7 % selectivity for methane, and 42.3 % CO conversion under conditions of 340°C, 2.0 MPa, and $H_2/CO = 2.7$ [119,120].

A series of Li-promoted $FeMnMgO_x$ catalysts was synthesized using co-precipitation and impregnation methods to evaluate the impact of promoters on iron phase evolution, chemisorption, and FTO performance. Mg enhances dissociative CO adsorption, disperses $\alpha$-$Fe_2O_3$, and suppresses carbonization, leading to higher light olefin selectivity. Meanwhile, Li promotes CO conversion and the formation of the x-$Fe_{2.2}C$ phase, resulting in decreased $CO_2$ and increased light olefins, with the FeMnMg-0.75Li sample achieving the highest space time yield of 355 g/(kg$_{cat}$.h) [121].

- **Transition Metals as promoters**

  Mn-Fe and Zn-Fe oxides catalysts have been employed as bimetallic catalysts for olefin production by the co-precipitation method. It is noted that Mn and Zn enhance olefin selectivity by increasing surface area and dissociative CO adsorption on the catalyst surface while reducing $H_2$ adsorption and carbon deposition [96,122,123]. A novel structure of a manganese (Mn)-modified $Fe_3O_4$ catalyst was assessed in a study, where $MnO_x$ is dispersed on the surface of $Fe_3O_4$ microspheres. This modification enhances the catalyst's porous structure and alters its carburization process, aiming to effectively convert syngas into light olefins. This catalyst improves the selectivity of light olefins by reducing secondary reactions. The presence of Mn led to the formation of a unique $\theta$-$Fe_3C$ carbide phase on the $Fe_3O_4$ microsphere surface, and the formation of $\theta$-$Fe_3C$, which was associated with enhanced selectivity for light olefins. According to that, by addition of Mn promoter to $Fe_3O_4$ catalyst (3 wt% and 6 wt %), methane selectivity decreased, and light olefin selectivity increased; however, by increasing loading of Mn up to 12 wt%, the number of active sites of Fe decreased, resulting in weaker catalyst performance. As the Mn content exceeds the optimal range, the balance of active sites and their composition can shift, potentially favoring other reaction pathways [111]. Four different catalysts were prepared by physically mixing Fe powder ($\alpha$-$Fe_2O_3$) and Mn oxide ($MnO_2$) in varying ratios: $\alpha$-$Fe_2O_3$, $MnO_2/\alpha$-$Fe_2O_3 = 0.5$, $MnO_2/\alpha$-$Fe_2O_3 = 1$, and $MnO_2/\alpha$-$Fe_2O_3 = 2$. Among these, the pure $\alpha$-$Fe_2O_3$ catalyst showed the highest CO conversion but lowest light

olefin selectivity and methane selectivity. The conversion decreased during the reaction due to the formation of the graphitic carbon layer. The addition of $MnO_2$ improves the performance of catalysts for light olefin production to some extent because it changes the electronic structure of the catalyst. Increasing the $MnO_2/\alpha$-$Fe_2O_3$ ratio up to 2 altered the methane selectivity from 13.4 % to 18.6 % and decreased the light olefin selectivity from 51.1 % to 41.4 %. Fe carbide ($\theta$-$Fe_3C$) was formed due to the interaction of Fe and Mn, and its amount depended on the amount of loaded Mn. Moreover, the selectivity of light olefins was highly dependent on the content of $\theta$-$Fe_3C$ [124]. The use of Cu in Fe-Mn catalysts not only increases the conversion of CO and the selectivity of light olefins but also decreases $C_{5+}$ selectivity. As a sequence, the addition of Cu shifts the product distribution towards light olefins. This effect is attributed to Cu's overall weakened surface basicity, and although more $CH_x*$ intermediates are formed, their faster desorption results in a lower chain growth probability. The presence of Cu increases the amount of H* on the catalyst surface. This is important for facilitating various reactions, including chain propagation and termination steps. The higher coverage of H* contributes to improved catalyst activity [125].

The presence of zirconium (Zr) has both positive and negative effects on catalyst stability. Small amounts of Zr can lead to catalyst deactivation due to interactions that disturb previously existing interactions, resulting in the agglomeration or sintering of active nanoparticles. However, higher Zr/Fe ratios can lead to the formation of new Fe-Zr interactions that enhance stability, prevent sintering and aggregation, decrease CO conversion, and increase light olefin selectivity by raising the ratio to some extent, which is considered an optimum point. However, further increasing the ratio, adversely influences the performance of light olefin selectivity because of the inhibition effects of the $ZrO_2$ species on the surface. The new Fe-Zr interaction that forms with increased Zr content could hinder the reduction of $Fe_2O_3$, resulting in higher reduction temperatures and lower catalytic activity [110]. The presence of Na in Fe-Zr catalysts enhances the activity more; however, there is an optimal point for Zr addition[126].

Porous catalyst materials such as $Fe_3O_4$ microspheres are useful in the FTO process to control chain growth and product selectivity. Also, Ag is an effective promoter for Fe-based catalysts' activity and selectivity. The addition of Ag was found to promote the formation of microspheres consisting of $Fe_3O_4$ nanoparticles when studying the influence of introducing different Ag contents as a promoter to porous $Fe_3O_4$ microspheres on the catalyst activity. Ag nanoparticles act as seeds for the aggregation of adjacent $Fe_3O_4$ nanocrystals in a common crystallographic orientation, which, Ag-promoted porous catalysts showed higher yields of olefins and low $CH_4$ selectivity than unmodified Fe catalysts [127].

- **Nonmetals**

  In the case of Co-based catalysts, Co, $Co_2C$, and $Co_3C$, are the active sites that determine the selectivity of light olefins in the FTS reaction catalyzed by Co [87,128]. It's worth mentioning that the indirect light olefin production performance is entirely different than that of the typical Co-based FT catalyst. In a typical FT catalyst, the active site is considered to be metallic Co, but in direct conversion, the active site is Co carbide ($Co_2C$) and can be changed by operating conditions [3,129]. The transition from $Co_2C$ nanoprisms to metallic CoO and $Co_2C$ nanospheres, as well as the formation of $Co/Co_2C$ interface, plays a crucial role in determining the selectivity and distribution of products in the catalytic process. Operating conditions influence the product distribution in the syngas conversion to hydrocarbons process by affecting the morphology of $Co_2C$. Reduction conditions, such as temperature and composition of the reducing agents, play a crucial role in control the morphology of $Co_2C$ nano-catalysts [130]. For instance, the particle size of Co carbide is an effective parameter for controlling catalytic activity. When $Co_2C$

nanoparticle size exceeds a specific threshold, catalyst activity and product selectivity are supposed to be independent of size. Conversely, as size decreases, catalyst activity, olefin selectivity, and the olefin-to-paraffin ratio tend to increase, while methane selectivity decreases. Smaller catalyst sizes result in increased surface area and energy per unit mass, providing more active sites for catalytic reactions [130,131].

Promoters can also affect the performance of Co-based catalysts. S is commonly used promoters to enhance the catalyst [132]. One contentious approach to improve FT catalysts involves incorporating trace amounts of S to enhance their stability. This method has been extensively studied, and consensus suggests that catalysts have specific thresholds for S tolerance, as excessive S loading can lead to surface poisoning where S species occupy active sites on the catalyst surface. This prevents reactant molecules from adsorbing and reacting effectively, reducing the overall catalytic activity. S poisoning can block essential reaction pathways and inhibit the formation of desired products [133]. For example, a study based on the CoMn$_3$-Na$_2$S$_2$O$_3$ catalyst showed a high C$_2$-C$_4$= olefins selectivity of about 54 % and a low methane selectivity of 17 %, which is lower than what was predicted by the ASF distribution [90]. S is also effective additive that has been shown to enhance the Fe- based catalyst activity and product selectivity, as reported by Yuan et al. [134].

- **Mixed metals**

The effect of Zn, Si, and Ti as structural promoters on Fe catalysts' structure and catalytic performance for light olefins' direct synthesis from syngas was studied. Results showed that adding Zn to Fe bulk catalyst enhances the catalytic activity and light olefin selectivity. Zn acts by improving CO conversion, retarding the WGSR, and creating favorable surface chemistry that weakens the bonding between Fe and carbon atoms. This weakening enhances the desorption of olefins while reducing the secondary reactions that convert olefins into paraffins. In contrast, Ti and Si additions adversely affect catalyst performance, decreasing CO conversion and light olefin selectivity. The negative impacts are created by disrupting active site formation, leading to particle agglomeration and reduced CO conversion and

light olefin selectivity. Unlike Zn, which forms beneficial crystal phases (ZnFe$_2$O$_4$ and ZnO), do not form clear crystal phases of Fe oxides, further contributing to their detrimental effect. This suggests that the introduction of Ti and Si might disrupt the formation of well-defined active sites crucial for the desired catalytic reactions, leading to larger particle agglomerates, reduced surface area, and lower catalytic activity. On the other hand, adding Al as a promoter improves the catalytic activity but decreases the light olefin selectivity, making Zn the superior promoter among unsupported Fe catalysts [135]. However, despite improvements, these unsupported catalysts exhibit high selectivity for gasoline over light olefins, making them less suitable for light olefin production from syngas [136].

- **Post transition Metals as promoters**

Lead (Pb) and bismuth (Bi) are effective promoters known for their ability to exist in multiple oxidation states and undergo easy redox cycles between metal and oxide forms. FeC$_x$ promoted catalysts exhibit a 5−10-fold increase in the FT rate and achieve light olefin selectivity of up to 60 % compared to unpromoted catalysts. Additionally, Bi- and Pb-promoted catalysts enable the selective production of light olefins from syngas with high yields at atmospheric pressure. The presence of these promoters enhances the intrinsic activity of iron carbide active sites, likely by facilitating CO dissociation through the removal of oxygen [114].

The light olefin and methane selectivity, and CO conversion for conventional FT catalysts have been shown in Fig. 6.

### 3.1.2. Effect of supports on the performance of Fe-based catalysts

Promoter-containing bulk catalysts stand out as attractive catalyst candidates for the FT-Olefin process due to their high light olefin selectivity, low methane production, and high conversion. However, unsupported Fe catalysts undergo significant mechanical degradation in FT applications, especially when high CO-containing syngas is fed above 300°C. One way to overcome this problem is to load the desired catalyst material on a support material. Dispersing the catalyst used for the FT-Olefin process on a support material prevents the catalyst particles from coalescing and aggregating under FT operation conditions, thus helping
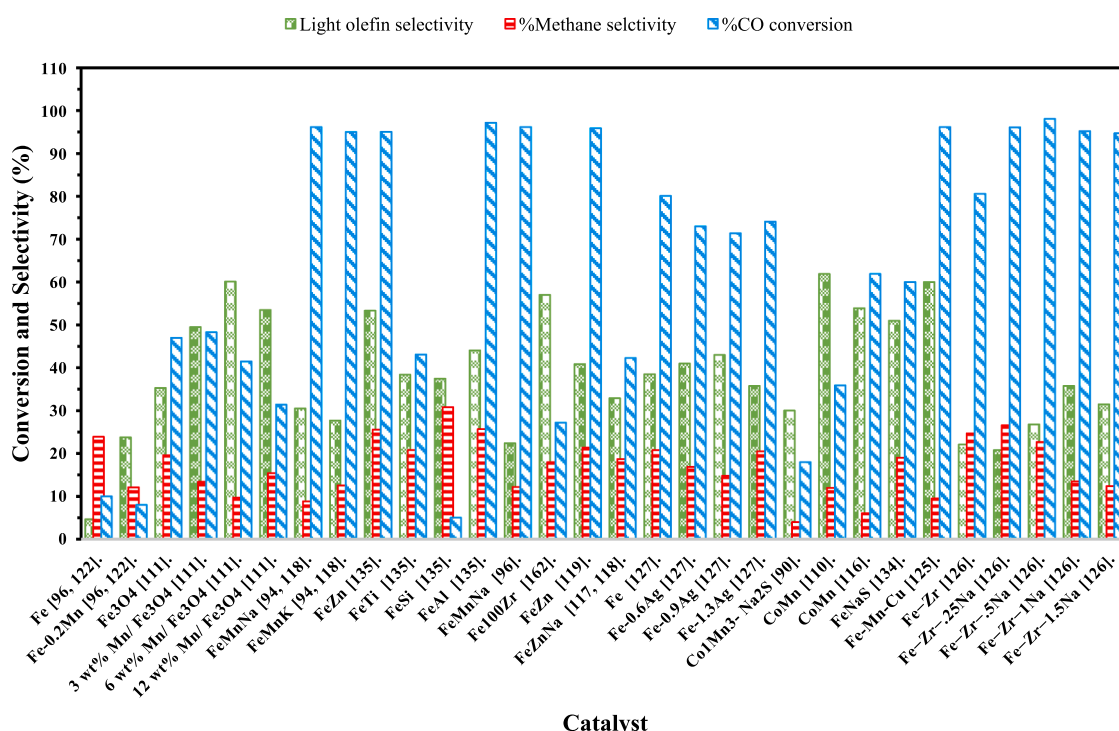


**Fig. 6.** Light olefin and methane selectivity, and CO conversion with promoted unsupported catalysts.

to ensure the stability of the catalyst. Using porous supports for catalysts increases the surface area, improves the dispersion of the active metal phase, and enhances catalytic performance via a positive interaction between metal nanoparticles and the support, which limits sintering [135,137]. The mechanism of supported FTO catalysts involves the adsorption and dissociation of syngas on metal active sites (such as Fe, and Co) dispersed on a support material (e.g., silica, alumina, AC, CNTs). CO molecules dissociate into carbon and oxygen atoms, while $H_2$ provides hydrogen atoms, forming surface-bound $CH_3$ species. These species react with additional CO and $H_2$, propagating hydrocarbon chain growth through the stepwise addition of $CH_2$ units. Chain termination occurs via beta-hydride elimination, resulting in the formation of olefins or paraffins, which then desorb from the catalyst surface. The support material enhances the dispersion and stability of the active metal, while promoters and reaction conditions (temperature, pressure, and $H_2$/CO ratio) influence the catalyst's activity and selectivity, optimizing the conversion of syngas to desired hydrocarbons [138–140].

Catalytic supports can also be efficient in increasing the mechanical stability of metal-based catalysts. Many different support materials have been used for this purpose to produce light olefins. The support material's mechanical strength, morphology, and porosity are important factors to consider in catalyst design. The support material stabilizes the Co and Fe nanoparticles and improves the activity and stability of the FT catalyst. The surface structure and pore diameter of the support material have a decisive effect on the metal dispersion, the reducibility of the metal, and the diffusion coefficients of the reactants and products [141–143]. Key considerations in selecting support materials include achieving optimal dispersion of the active phase, enhancing heat and mass transfer, stabilizing against morphological changes and surface area losses, and providing mechanical strength. The surface area and pore structure of the support material control reducibility, dispersion, and morphology of the active phase, thus decisively impacting catalytic performance. The size, distribution, and shape of the pores in the support material determine the diffusion resistance of the reagents and products. The interaction between the metal and support material is another critical parameter in support selection; weak interactions may result in poor dispersion of the active phase, while overly strong interactions, such as Co, Fe-aluminate, or silicate formations, can reduce catalyst reducibility and activity (Fig. 7) [136,144].

Among these, core-shell catalysts represent a distinct subclass where a core material (active phase) is encapsulated by a shell of a different material (zeolite or metal oxide). This unique structure offers several advantages, such as protection of the core, enhanced catalytic activity, and improved selectivity. Due to the porosity in its structure and the acidic characteristics of the zeolite shell, it can enhance the selectivity of products. The core of the catalyst produces the weighty hydrocarbons, and in the next step, these long-chain hydrocarbons can be cracked to form different hydrocarbons when their diffusion takes place by passing through the shell (based on shell type)[146]. Zeolite shell and the combination of core and shell can be synthesized by hydrothermal and co-precipitation methods, respectively [147]. These kinds of catalysts have been considered by researchers for light olefin production from syngas due to the mentioned properties. Fig. 8 shows the structure of core@shell catalysts.

Numerous studies have been devoted to investigating the effects of different supports. Historically, researchers have predominantly used
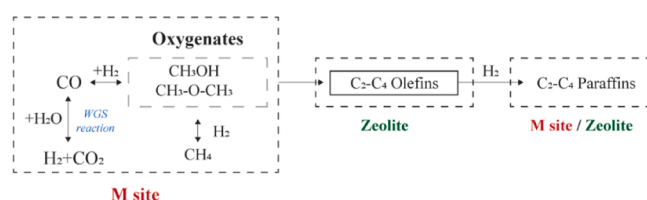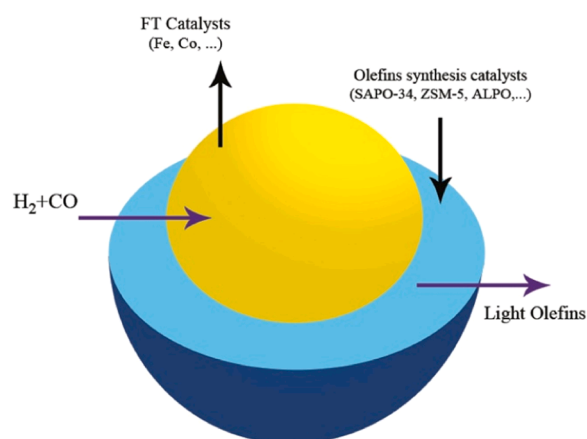
**Fig. 8.** Structure of a core@shell catalyst [147].

$Al_2O_3$, silica ($SiO_2$), CNT, and zeolites as supports for FTO catalysts [144, 148]. The catalyst properties are affected by the average pore size and pore size distribution of the supports. Thus, the modification of supports dramatically influences the performance of the catalyst [149]. With $Co/Al_2O_3$ catalysts, increasing pore size enhances the dispersion of the active phase, and the catalyst's activity depends more on the pore structure than the $Al_2O_3$ phase. Additionally, higher surface areas of $Al_2O_3$ correlate with decreased $C_{5+}$ selectivity [150]. On the other hand, supporting the Co catalyst with $SiO_2$ can form larger Co crystallites, which indicate lower dispersions and easier reductions [151]. To produce light olefins from syngas, conventional FT catalysts have been supported by zeolites, metal oxides, CNTs, and graphene oxides.

• **Oxide-supported/ shell catalysts**

Based on previous sections, the strong and efficient interactions between metals and supports make Fe and Co catalysts supported on $SiO_2$ or $Al_2O_3$ promising candidates for commercial FTO processes [152,153]. According to theoretical research and density functional theory, oxygen vacancies in metal oxides significantly affect syngas activation. Considering this factor, it will provide new insights into catalyst design [154]. In this section, metal oxide-supported catalysts for the FTO process have been reported.

Fe catalysts promoted by Bi and Pb have demonstrated high light olefin selectivity. The secondary hydrogenation of olefins to alkanes leads to an increase in $CO_2$ selectivity and a decrease in light olefin selectivity for an unpromoted Fe over $SiO_2$ catalyst. The addition of Pb and Bi promoters increased light olefins selectivity and exhibited a lower selectivity for long-chain hydrocarbons by modifying the intrinsic activity (turnover frequency) of the active sites and exhibiting mobility during the reaction, with evidence of migration and interaction with Fe carbide nanoparticles [114].

The CO conversion and selectivity to $C_2$-$C_4$= olefins initially increase with the addition of $MnO_x$ to the Fe/$SiO_2$ catalyst, reaching a maximum value. This occurs because $MnO_x$ promotes the reduction of $Fe_2O_3$ to $Fe_3O_4$, which is a crucial precursor for active Fe carbide formation. However, with higher $MnO_x$ content, both CO conversion and olefin selectivity decline. Excess $MnO_x$ may inhibit Fe activity by covering active sites. The chain growth probabilities ($\alpha$) increase slightly with $MnO_x$ addition, leading to enhanced selectivity towards lower olefins [155].

Ce and Zn are two effective promoters for the FTO process. For the Co-Mn/$SiO_2$ catalyst, these promoters improve CO conversion and $C_{5+}$ selectivity, decrease $CO_2$ and methane selectivity, but reduce light olefin selectivity, making them less suitable promoters for light olefin production when added to Co-Mn/$SiO_2$ catalyst. This is attributed to the restraint of hydrogenation reactions and an enhancement in chain

**Fig. 7.** Role of supports for catalysts [145].

propagation reactions [156]. By adjusting synthesis condition parameters such as achieving a specific surface area exceeding 300 $m^2.g^{-1}$, a pore diameter greater than 6 nm, a pore volume surpassing 0.36 $m^3.g^{-1}$, ensuring a broad distribution of pore sizes, and establishing a mesoporous structure, the selectivity of the Co-Mn/SiO$_2$ catalyst towards specific products can be influenced. These conditions have been optimized to achieve the highest possible rate of production for light olefins [157].

The initial crystal structure of Fe$_2$O$_3$, Mn addition, and presence of different carbide structures ($\alpha$-Fe$_2$O$_3$ and $\gamma$-Fe$_2$O$_3$) affect the catalyst activity. The addition of Mn to the $\alpha$-Fe$_2$O$_3$ and $\gamma$-Fe$_2$O$_3$ creates surface Fe species, altering the product selectivity and mitigating diffusion limitations during the FTS reaction [158]. The impacts of Na and S on Fe catalysts supported by $\gamma$-Al$_2$O$_3$ were shown that an unsupported Fe catalyst had high methane selectivity and low light olefin selectivity. By adding S and Na to bulk Fe catalysts, the selectivity of light olefins was substantially enhanced (by 60 %), although this significantly impacted coke formation. Al$_2$O$_3$-supported catalysts improved light olefin selectivity with S as a promoter compared to Na. This is because S weakens the Fe-CO bond, potentially enhancing catalytic activity by increasing surface reactivity. Na, on the other hand, improved chain growth probability but sometimes strengthened the Fe-CO bond, which could reduce catalytic activity. The combination of Na and S with the same ratio gave the best performance, as Na helped stabilize and anchor S while S weakened the Fe-CO bond, leading to increased activity and selectivity for light olefins [91]. The addition of Ba to Co/Al$_2$O$_3$ enhances the surface basicity of the catalyst due to the Ba's alkaline nature. This shift affects the interaction between CO and the catalyst surface, favoring CO adsorption and dissociation. Enhanced CO adsorption and dissociation due to the presence of Ba improves selectivity towards heavier hydrocarbons [159].

Ni and Cu additions to the Al$_2$O$_3$ increase light olefins selectivity. However, a significant limitation of using these metals as bulk catalysts is their deactivation at high temperatures due to the coke formation covering the catalyst surface. Using metals over Al$_2$O$_3$ support enriches catalyst activation [160].

The use of K derived from chloride precursors in catalytic reactions has shown remarkable improvments in light olefins selectivity. K plays a crucial role in enabling the preferential synthesis of light olefins, coupled with a substantial conversion of CO. This effect is particularly pronoounced with syngas compositions similar to those derived from biomass sources. The presence of chloride increases the selectivity for C$_2$-C$_4=$ olefins. The promotional effect of chlorine is attributed to an increase in the C/H ratio on the catalyst surface, favoring the desorption of olefins over paraffins [161].

Efforts to optimize catalyst behavior by adding two promoters have shown that while a single promoter improves catalyst stability, the addition of two promoters not only enhances stability but also improves consistency in CO conversion. The ratio of olefin selectivity to paraffin increased from a non-promoted catalyst to a single-promoter catalyst, reaching its maximum with a double-promoted catalyst. Methane selectivity decreased during tests with Fe-based catalysts [162].

Activity is not the sole consideration; stability is another crucial characteristic of a catalyst. For instance, Fe-based catalysts with different supports, such as $\beta$-SiC, CNFs, $\alpha$-Al$_2$O$_3$ and $\gamma$-Al$_2$O$_3$ were studied. Fe/$\alpha$-Al$_2$O$_3$ exhibited lower initial activity compared to Fe/$\beta$-SiC and Fe/CNF. However, Fe/$\alpha$-Al$_2$O$_3$ demonstrated excellent resistance to deactivation and maintained stability. The use of CNF and $\alpha$-Al$_2$O$_3$ as supports resulted in the uniform distribution of Fe oxide particles, contributing to efficient activation and optimal catalytic performance. Both Fe/CNT and Fe/$\alpha$-Al$_2$O$_3$ are preferred for producing light olefins (>50 % C) with lower methane production (<15 % C) [17, 163].

In another study, Co-based, magnesium and Na-promoted, CNT, $\gamma$-Al$_2$O$_3$, and SiO$_2$ supported catalysts have been synthesized in a research. For significant light olefin production over a Co-based catalyst,

the formation of Co$_2$C is crucial, reqquiring a relatively weak interaction between Co and the support. The CoMnNa/SiO$_2$ catalyst exhibited superior light olefin selectivity over other supported catalysts because it generates desirable Co$_2$C nanoprisms with exposed facets, leading to enhanced olefin selectivity. Regarding the P/O ratio, CNT support performed better, while $\gamma$-Al$_2$O$_3$ was considered the best support for CO conversion [164].

The method of catalyst preparation impacts both the structure of the catalyst and the distribution of the resulting products. The impact of two preparation methods, including thermal decomposition and impregnation for Co-Mn/Al$_2$O$_3$ catalyst, has been investigated. Significantly improved outcomes have been achieved using catalysts produced through thermal decomposition compared to those prepared via the impregnation technique. The thermal decomposition method results in smaller particle sizes, higher dispersion, and a improved surface area, all of which contribute to increased catalytic activity [165].

However, the presence of S on the catalyst surface can sometimes hinder the reduction process. S can absorb onto the catalyst's active sites, blocking access to H$_2$ molecules, and hindering the effective reduction of Fe catalyst. Comparing two types of catalysts, including Fe/$\alpha$-Al$_2$O$_3$ and S$_{0.005}$Fe/$\alpha$-Al$_2$O$_3$, revealed that operating temperature had an extensive impact on S-modified Fe catalysts. For instance, the initial CO conversion for S0.005Fe/$\alpha$-Al$_2$O$_3$ was lower compared to Fe/$\alpha$-Al$_2$O$_3$. However, they achieved similar levels when the temperature was raised from 310°C to 350°C, indicating accelerated reaction rates due to increased thermal energy providing sufficient activation energy for reactant molecules. Conversely, S-modified Fe catalysts produce fewer olefins compard to non-S catalysts, indicating that elevated temperatures can mitigate but not completely eliminate the negative effect of S [166].

Calcination conditions significantly influence the catalyst's physical properties, particle size, and performance. Catalysts calcined in air typically exhibit smaller particle sizes, higher reducibility, and better activity compared to those calcined catalyst by argon. Air-calcined catalysts also show increased methane selectivity, light olefin selectivity, and CO conversion due to enhanced reducibility, a larger specific surface area, and reduced carbon deposition [167].

In core@shell catalysts, the shell thickness is a critical factor affecting product distribution. The modified Stöber method is a fruitful technique for the preparation of the core@shell catalyst due to its higher control over shell thickness. The higher olefin selectivity and O/P ratio are achievable by introducing the SiO$_2$ shell to the FeMn catalyst and also by optimizing the shell thickness. The SiO$_2$ shell acts as a confinement medium that can influence the residence time of reaction intermediates and products near the active sites and enhance the adsorption of H$_2$, increasing the local concentration of hydrogen near the active sites. This increased hydrogen concentration can promote hydrogenation and chain termination reactions [168].

The activity of the catalyst depends on the dispersion and reducibility of active Fe sites. For example, Fe@SiO$_2$-graphitic carbon (GC) core@shell catalyst synthesized using the hydrothermal deposition method show improved performance. The presence of GC modifiers and their interaction with Fe oxide species lead to the reduction of Fe oxides to metallic Fe and Fe carbides. These reduced phases are known to be active for FT synthesis and promote the formation of olefins. Over the catalyst test, the lower olefin selectivity increased to 39.07 % for Fe$_2$O$_3$@SiO$_2$, 40.69 % for Fe@SiO$_2$-GC-1 (2.5 g polyvinylpyrrolidone (PVP)), 37.42 % for Fe@SiO$_2$-GC-2 (5 g PVP), and 37.42 % for Fe@SiO$_2$-GC-3 (7.5 g PVP). PVP content as a stabilizer is vital in the mentioned catalyst, preventing the agglomeration of Fe nanoparticles during catalyst synthesis and contributing to the formation of a mesostructured SiO$_2$ shell through self-assembly. However, an excessive amount of PVP can lead to undesirable effects, potentially affecting the uniformity and dispersion of Fe species and resulting in an incomplete or less effective shell formation [169].

In summary, metal oxide-supported Fe and Co catalysts are

promising for the FTO processes due to their strong interactions with supports and strategic use of promoters. Effective catalyst design and preparation methods are critical for achieving high selectivity for light olefins. For details on catalyst performance, including light olefin, and methane selectivity, CO conversion, and operational conditions, refer to Fig. 9, and Table S1.

- **Active Carbon/ CNT-support/shell**

Nanocarbon materials, such as carbon nanofibers (CNF) and CNTs, are relatively novel supports for the direct synthesis of olefins from syngas [148,149]. When using CNTs as catalyst supports, the catalytic activity depends on the deposition of metal nanoparticles, whether inside or outside the nanotubes [170,171].

Surface modification with different functional groups (such as oxygen and nitrogen) changes the surface charge density, hydrophilicity, and reactivity of the catalyst. Zeta potential measurements and point of zero charge (PZC) values provide insights into the surface functional groups and their influence on the catalyst's electronic properties and reactivity. Nitrogen doping introduces basic sites on the NCNTs support, which enhances the adsorption of CO molecules and the reducibility of Fe species, facilitating the formation of active Fe carbide phases and the dispersion of Fe species on the catalyst support. Nitrogen-doped CNT is one CNT form that has been used as support for Fe nanoparticle catalysts for FTO reactions. In a study, this type of catalyst was synthesized by in situ chemical vapor deposition and purified, and NCNT-supported Fe catalyst (Fe/NCNT) was prepared by the incipient wetness impregnation method. FTS reactions were carried out under atmospheric pressure, 300°C, with an $H_2$/CO of 1 in a fixed bed microreactor. The CO conversion and selectivity for light olefins increased with Fe loading from 2 to 10 wt % (CO conversion: 4–14.4 %; light olefin selectivity: 28–46.7 %), but gradually decreased when Fe loading exceeded 10 wt% (CO conversion: 14.4–10 %; light olefin selectivity: 46.7–38 %). Therefore, an increase in Fe content is beneficial only up to a certain point where the active sites become saturated. Further increase in Fe content doesn't significantly contribute to the reaction rate and can lead to the aggregation and growth of Fe particles [172].

Pristine, close-packed multiwalled CNTs (MWCNTs (p-CNTs)) can be oxidized under various conditions to produce different supports for Fe-based catalysts, with diameter ranging from 10–15 nm. These include high-temperature pretreatment of CNT (HT-CNT), nitrogen-doped CNT (N-CNT) mesoporous carbon, and O-functionalized mesoporous-carbon supported catalyst. Differences in surface roughness and integrity between different supported catalysts (Fe/O-CNT, Fe/N-CNT, Fe/HT-CNT) can influence the interaction between the catalyst and reactants. Among these supports with low Fe loading, Fe/HT-CNT exhibits the highest light olefin selectivity despite showing weak CO conversion. Fe/HT-CNT has an electron-withdrawing effect on $Fe_3O_4$ nanoparticles, which is likely due to the presence of defects and other modifications on the HT-CNT surface. This electronic effect on $Fe_3O_4$ nanoparticles contrasts with the electron-donating effect observed for other carbon supports with oxygen or nitrogen functionalities [173].

Though K, Na, and Mn promoters have been preferred in many studies for supported and unsupported Fe catalysts, other important promoters have been utilized as novel materials to increase the yield of valuable chemicals. For instance, Bi and Pb can be incorporated into Fe-based catalysts supported on CNTs. They are typically prepared by initially impregnating the CNT support via incipient wetness with Fe, followed by introducing Pb and Bi through co-precipitation from their respective precursors. Based on research, the CO conversion and stability of catalysts have been ranked as Fe/CNT < FeBi/CNT < FePb/CNT. As pressure decreases, the addition of promoters increases the selectivity for light olefins, as light olefin production is favored at lower pressures (the ranking for selectivity is Fe/CNT < FePb/CNT< FeBi/CNT). Promoters (especially Pb) migrate to the surface of Fe carbide nanoparticles during the reaction, forming a shell of promoter over the Fe carbide core. This close contact between Pb and Fe enhances Fe carbidization and promotes CO dissociation on the Fe carbide surface [174,175].

The configuration of the Fe nanoparticles encapsulated with CNT support is another effective parameter influencing catalyst performance. When the active phase is located inside the CNT, the catalyst tends to yield more light olefins compared to activated carbon and
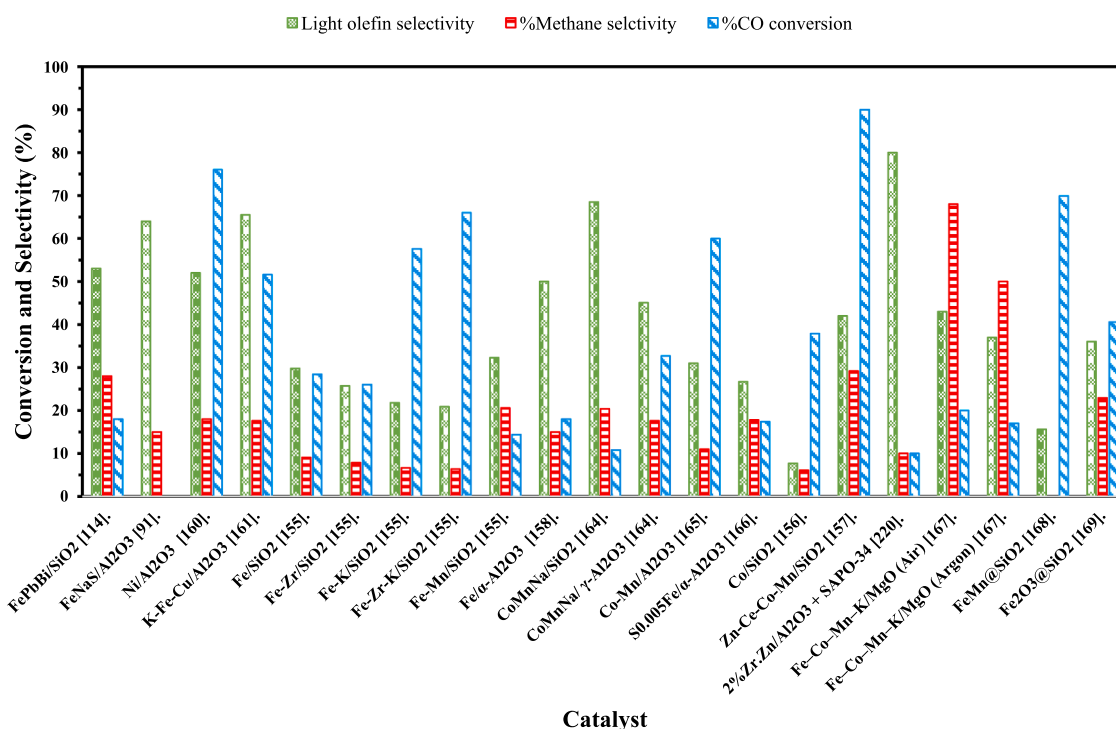
**Fig. 9.** Light olefin and methane selectivity, and CO conversion with oxide supported catalysts.

CNTs with the active phase outside (CNT-out). The restricted growth of Fe oxide nanoparticles inside CNTs, limited by the CNT diameter, helps maintain smaller and more active Fe crystallites. The confinement of Fe nanoparticles within CNTs also improves the stability of the catalyst, allowing it to maintain its activity over a longer period. This enhanced stability is likely due to the reduced sintering of Fe carbide nanoparticles when confined inside the CNTs [176]. The presence of Bi significantly increases the catalytic performance of the Fe catalyst. Bi undergoes redox cycles during catalyst activation and FT synthesis. Bi oxide ($Bi_2O_3$) present in the catalyst is reduced to metallic Bi during activation in CO. The reduction of Bi from oxide to metal enhances its mobility and interaction with the Fe carbide active phase. This redox behavior of Bi contributes to its promoting effects on the catalyst [177,178]. The Na promoter was found to increase activity and selectivity for light olefins, with improved stability being another significant advantage. However, a drawback of Na-promoted catalysts is their tendency to sinter over time. After 100 h, the promoted catalyst's activity initially matched that of the unpromoted catalyst. Furthermore, larger particle sizes led to increased sintering, resulting in decreased activity and stability; this effect was expected to be less pronounced in unpromoted catalysts. Hence, stability and activity can change with both time and particle size. To enhance olefin yield, specific promoters should be considered, along with strategies to mitigate deactivation [179].

Carbon fiber, pure carbon, graphite, carbon black, and active carbon (AC) can be used as supports for bimetallic FeCu catalysts promoted by K. Catalysts without support can achieve higher CO conversion rates, although they may face stability issues. The addition of K increases CO conversion across all catalysts, while reducing methane selectivity to below 5 %. Under optimal operating conditions, FeCu-K/AC demonstrates higher CO conversion and STY compared to other catalysts on account of the more surface area provided by active carbon, which helps the Fe disperse better and provide more active sites to suppress the WGS activity. Ozone-treated active carbon is favored to enlarge pore diameters for significant olefin yield and the stability of the catalyst compared to the untreated catalyst. This treatment improves catalyst stability by suppressing the accumulation of heavy hydrocarbon products and leads to a better distribution of hydrocarbon products with higher carbon numbers [180]. Mn exhibits the best performance among Mn, V, Ti, K promoters for the FeCu/AC catalyst, helping to suppress the secondary hydrogenation of olefins in favor of jacobsite ($MnFe_2O_4$) formation, contributing to the catalytic behavior. When using FeCuMn/AC, increasing the $H_2$/CO ratio up to 4 results in a rise in light olefin selectivity. This is due to weakened hydrogen adsorption, which restricts hydrogen availability for secondary hydrogenation reactions, thereby suppressing the hydrogenation of olefins to paraffins. These findings contrast with those observed with the unpromoted catalyst, where higher surface hydrogen concentrations promote olefin hydrogenation, resulting in decreased olefin selectivity [181,182].

Alkali metal promoters are known to influence the adsorption and activation of reactant molecules on the catalyst surface, leading to changes in reaction pathways and selectivity. An important aspect concerning alkali metal promoters, such as Na and K is that Na addition appears to inhibit hydrogenation reactions, leading to an increase in olefin selectivity and CO conversion. K, on the other hand, increases light olefin selectivity but also leads to a decrease in CO conversion and overall activity [183].

In conclusion, nanocarbon materials such as CNF and CNTs are promising supports for olefin synthesis from syngas. Functional modifications, including nitrogen doping, enhance catalytic properties by improving CO adsorption and Fe species reducibility. Encapsulating Fe nanoparticles within CNTs maintains smaller, more active crystallites, boosting stability and activity. Promoters such as

Bi, Pb, Na, and Mn significantly affect Fe carbide formation and CO dissociation, tailoring the catalyst's performance towards desired products. Various carbon-based supports, like AC, enhance metal dispersion and catalytic efficiency, with treatments like ozone optimization further improving stability and olefin yield. Overall, optimizing support materials, surface modifications, and promoter additions is crucial for developing efficient and stable catalysts for industrial olefin synthesis.

- **Graphene oxide-support/shell**

Incorporating FT metal catalysts into graphene oxide enables them to function as FTO catalysts. It has been proven that remnant oxygen species in graphene oxide can repress methane production in FTO reactions. Supported Fe-based catalysts with promotion can enhance catalyst activity. In a study, a K-promoted Fe-based catalyst supported on reduced graphene oxide (rGO) was evaluated. Varying amounts of K were incorporated into the catalysts (Fe/rGO, FeK0.5/rGO, FeK$_1$/rGO, FeK$_{1.5}$/rGO, FeK$_2$/rGO); FeK$_1$/rGO achieved the maximum Fischer-Tropsch yield (FTY); while FeK$_2$/rGO showed the highest potential for producing light olefins and reducing methane and paraffins [184]. In another study, incorporation of different metals (K and Mn) with microwave irradiation (MWI)-assisted reduction methods on Fe-based-reduced graphene oxide-supported catalysts have been investigated, and the results showed that these catalysts could be claimed to lead to the production of longer-chain hydrocarbons due to the presence of the $Fe_5C_2$ (Hägg Fe carbide) active phase, which is known for promoting chain growth. This active phase favors the addition of carbon atoms to existing hydrocarbon chains, leading to longer-chain hydrocarbons [185].

To compare the performances of Mn-promoted Fe-based catalysts and Mn-free Fe/rGO catalysts, the selectivity for $C_{9+}$ was acutely reduced with an increase in Mn content. Based on the results, the CO conversion was not significantly affected when the Mn/Fe molar ratio was 16/100 compared to the Mn-free sample. Additionally, light olefin selectivity increased with the addition of Mn, but changing the molar ratio of Mn from 100/16–100/29/00 showed only a slight increase [186].

As noted, Mn is a well-known promoter for graphene oxide-supported catalysts in the light olefin production process. Thus, bimetallic $Al_2O_3$-supported Co-Mn catalysts with the various Co to Mn ratios (1:1, 1:2, 1:3, 2:1, and 3:1) were tested for CO hydrogenation of light olefins. The effect of the optimal ratio of graphene and reduced graphene oxide as supports was investigated after optimizing the Co/Mn ratio. The selectivity for light olefins varied with changes in supports (graphene oxide or reduced graphene oxide) and Co/Mn ratios. Using a Co/Mn ratio of 1 with reduced graphene oxide as a support minimized methane production and increased light olefin selectivity. This improvement was attributed to the higher specific surface area, porosity, and better dispersion of Co-Mn compared to the graphene nanosheets (GNS)-supported catalyst. The reduction process was used to prepare rGO and to introduce defects and functional groups into the graphene structure. These defects serve as nucleation sites for the formation of Co-Mn particles, leading to better interaction between the active phase and the support, enhancing reactant adsorption and facilitating catalytic reactions [187].

Graphene-like carbon-encapsulated Fe carbide catalysts with K as a promoter ($Fe_3C@C$) are another core@shell catalyst used for the FTO reaction. The unique graphene-like structure of the carbon shell enhances electron transfer and catalytic reactions on the catalyst surface, promoting selectivity towards olefins and preventing hydrogenation of intermediates. Small amounts of K doped into $Fe_3C@C$ catalyst enhance CO dissociation and create surface basicity, which helps suppress the hydrogenation of intermediates and the formation of alkanes, leading to increased selectivity towards light olefins. However, excessive K content can decrease CO conversion and catalytic activity due to factors like coking and competitive adsorption of $CO_2$, which can reduce the

availability of active sites [188].

In conclusion, incorporating FT metal catalysts into graphene oxide supports enhances their performance in FTO reactions by suppressing methane production. K-promoted Fe-based catalysts with rGO showed optimal results, with FeK1/rGO achieving the highest FTY and FeK2/rGO maximizing light olefin production while minimizing methane and paraffins. Microwave-assisted reduction methods improved these catalysts, favoring longer-chain hydrocarbon production due to the $Fe_5C_2$ active phase. Mn promotion increased light olefin selectivity without significantly affecting CO conversion. The optimal Co/Mn ratio and support type (GO/ rGO) influenced performance, with rGO showing better results due to higher surface area and improved Co-Mn dispersion. Graphene-like carbon-encapsulated Fe carbide catalysts with K promoter (Fe3C@C) enhanced light olefin selectivity, although excessive K reduced CO conversion. These results underscore the need to optimize catalyst composition and support materials for improved FTO reaction performance. Fig. 10 shows the performance outcomes of testing using carbon-based catalysts.

### 3.2. Bifunctional catalyst

Recently, researchers have focused on coupling two or more functionalities in a single catalyst particle—combining metal active phases for intermediate production with zeolites or zeotypes as support—for light olefin synthesis [189,190]. The acidity and structure of the zeolite significantlly affect the distribution of products in syngas conversion to light olefin [191]. Generally, in FTO reactions over zeolite-supported catalysts, the accepted pathway involves the adsorption and activation of CO molecules and the adsorption and dissociation of $H_2$ molecules over the active metal phase (at oxygen vacancies) to activate CO and $H^*$. This is followed by the formation of methanol intermediates, which then convert to light olefins over the zeolite support [192]. ZSM-5 and

SAPO-34 are the most commonly used zeolites. Paraffins/aromatics are typically the main products of the synthesis gas conversion. In this process, SAPO-34 zeolites increase the selectivity for light olefins to approximately 80 %. Also, a decrease in the Si content of SAPO leads to a slight increase in light olefins, with the maximum Olefin/Paraffin ratio [193,194].

Research focuses on the catalysis engineering of bi-functional catalysts for the one-step synthesis of liquid fuels from syngas. In this process, metal composite oxides activate CO molecules, followed by the formation of olefins at the acid sites of the combined zeolite/zeotypes molecular sieve (Fig. 11) [195].

For a unpromoted and a promoted Fe catalyst (Fe, FeP) combined with the pelletized H-ZSM-5 zeolite, the activity and selectivity of olefin obtained from the FeP catalyst are expected to be higher than those from the Fe catalyst due to the promotion effects of P. However, combining the P-promoted Fe catalysts with zeolite alters the catalytic activity
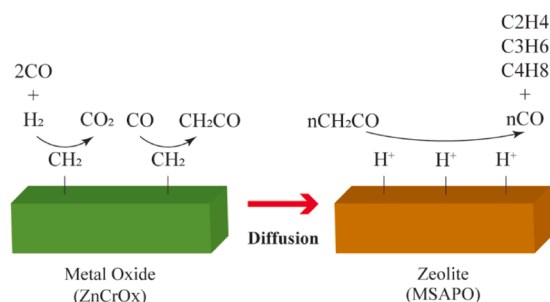
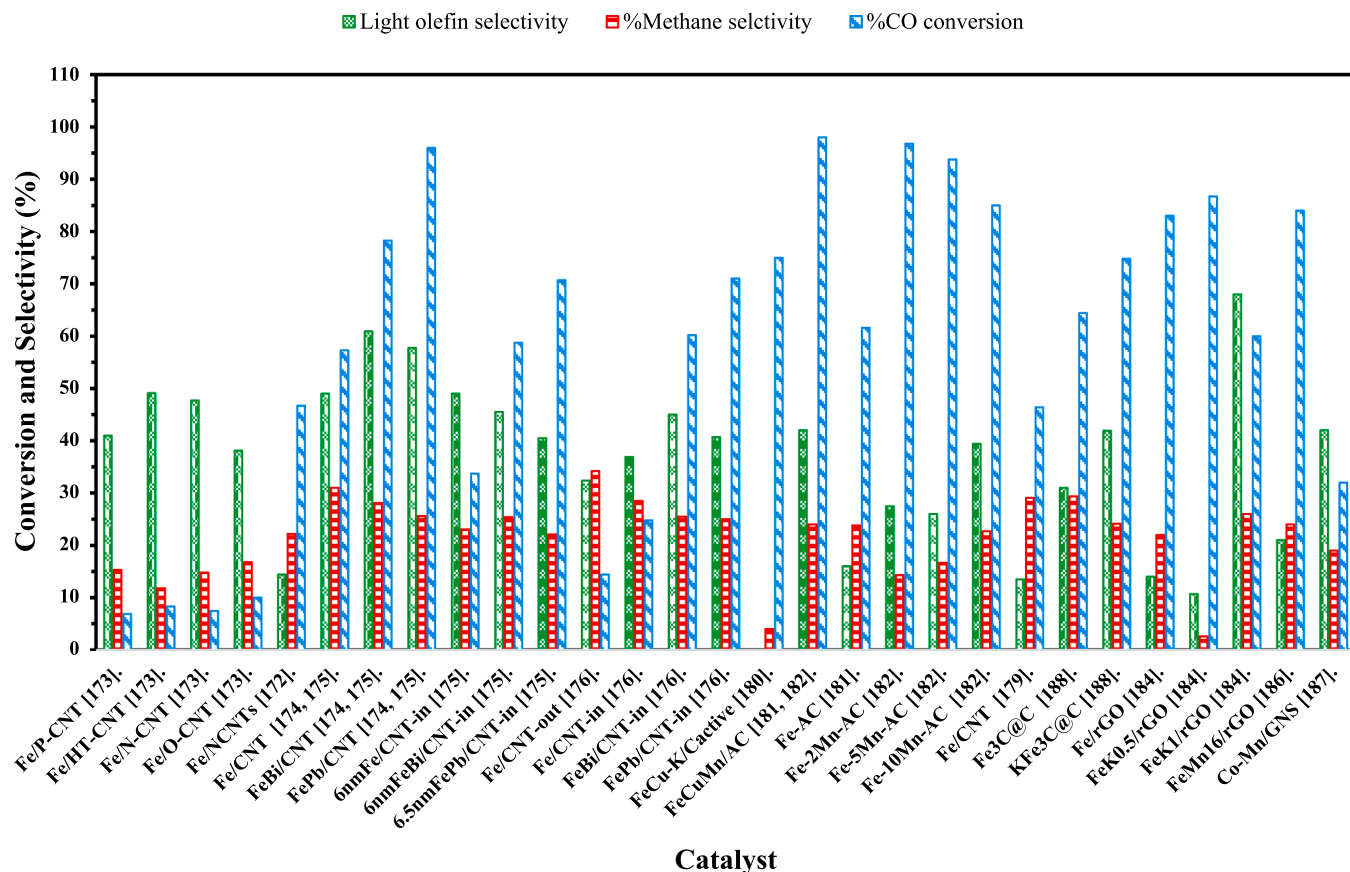**Fig. 11.** OX-ZEO bi-functional catalyst for direct production of olefins via syngas [195].

**Fig. 10.** Light olefin and methane selectivity, and CO conversion with carbon supported catalysts.

(catalytic activity increases when FeP-2Z (Z stands for zeolite and 2 is the ratio for $V_{zeolite}/V_{iron\ catalyst}$) is used as a catalyst). In contrast, a slight decrease in catalytic activity occurs in the combined Fe and zeolite catalyst (Fe-2Z) [196]. According to a research, the combination of Fe species with zeolite (Fe/HZSM-5 ($SiO_2/Al_2O_3=27$)) does not destroy the microporous structure of the zeolite. However, increasing Fe loading gradually covers the outer surface of the zeolite and partially blocks the zeolite micropores. Briefly, using an Fe catalyst without promoters leads the product distribution to $C_{5+}$ hydrocarbons and aromatics. Loading different amounts of Fe over HZSM-5 zeolites influences the catalyst acidity (decrease in Brönsted acid sites and increase in Lewis acid sites) and the performance of the Fe/HZSM-5 catalyst (enhancing the dehydrogenation property, promoting the selectivity of $C_{5+}$ hydrocarbons, and yielding aromatics) [197].

The deactivation of bi-functional catalysts is also influenced by support materials. For instance, an H-ZSM-5 supported Fe catalyst exhibits higher light olefin selectivity compared to one using CNT as support. When the Fe catalyst and zeolite are in proximity, Na ions from the Fe catalyst can migrate to the zeolite, leading to the neutralization of acid sites, and affecting its catalytic behavior. However, with the CNT-supported Fe catalyst, the migration of Na ions over the surface of the CNT support is hindered. This limitation in Na ions migration results in constant methane selectivity, suggesting that the CNT material restricts the charge compensation for Na ions. Aromatic selectivity is reduced by the promotion of Fe due to the loss of neutralizing acid sites in zeolite [198].

Operating conditions can greatly influence the catalyst's performance. A series of Co-HZSM-5 bifunctional catalysts with various Co loadings were prepared in a study. A dual-step reduction process of Co species occurred, with peaks corresponding to the reduction of $Co_3O_4$ to CoO and CoO to Co. Higher CO conversion and liquid hydrocarbon fuel production were observed over Co-HZSM-5 catalysts at lower space velocities. Increasing the space velocity to 1.5 L/(g.h) shifted the product selectivity from liquid hydrocarbons to gaseous $C_2$-$C_5$= olefins. High olefin selectivity at the higher space velocity was attributed to rapid desorption of intermediate olefins, preventing secondary reactions like hydrogenation and carbon insertion. Increased temperature and low $H_2$ concentration ($H_2$:CO = 1) resulted in increased O/P ratio and CO conversion, while higher temperatures led to increased methane selectivity without improving catalyst activity [199,200].

For forming light olefins, an aluminosilicate zeolite called SSZ-13 (having a chabazite (CHA)-topology like SAPO-34) can be considered an active component for selective intermediate binding. This zeolite has an equal and efficient function as SAPO-34 zeolite for the MTO reaction as well as for the selective catalytic reduction of $NO_x$ with $NH_3$ due to its high structural stability. $ZrO_2$ is helpful for CO activation; however, the Zn−O domains or small ZnO clusters are responsible for the activation of $H_2$, possibly by heterolytic dissociation. The Zr-Zn oxide and zeolite parts of the catalyst are active for methanol production and the MTO process, respectively. Using Zn-$ZrO_2$/SSZ-13 bi-functional catalysts enriches the selectivity of light olefins, reaching above 80 % [18,201]. Different combinations of Zr oxide catalysts have been developed, like InZr binary oxide with SAPO-34 zeolite and $ZnCrO_x$ with a mesoporous SAPO zeolite (MSAPO) as bi-functional catalysts to attain high light olefin selectivity and CO conversion [20,202]. In the case of $ZnCrO_x$/-SAPO-18 catalyst, the performance strongly depends on the Si/Al ratio in the zeotype. Increasing the Si/Al ratio raises the density of Brønsted acid sites and enhances their acidity strength, promoting secondary reactions of ethylene and increasing CO conversion. This is because more active sites are available at higher Si/Al ratios to catalyze the conversion of intermediates generated on the oxides [203,204].

The use of chromium (Cr) is considered environmentally less friendly; therefore, Mn oxide can be a good alternative to $ZnCrO_x$ due to its low price, environmental friendliness, superior redox activities, and oxygen storage properties, which can enhance light olefin selectivity up to 80 %. The presence of oxygen vacancies on the partially reduced Mn oxide surface is crucial for catalyzing the dissociation of CO molecules. These vacancies create active sites for CO activation and dissociation, leading to the formation of unidentifiable carbonate and carbon species on the catalyst surface. The $CO_2$ produced from the dissociation of carbonate species block the formation of surface oxygen species from CO, potentially reducing the need for the energy-intensive WGSR. Upon CO dissociation, surface carbon and unidentate carbonate species are formed on the Mn oxide catalyst surface. The active phase can exist in different oxide states: MnO, $MnO_2$, and $Mn_2O_3$. Optimal CO conversion and selectivity for light olefins are achievable by optimizing the reaction conditions and catalytic performance based on the mass ratios of $MnO_x$ and MSAPO [205,206].

Mn-Zr binary oxide catalysts combined with SAPO-34 zeolite as a support offer significant benefits for catalyst design. The use of Mn and Zr affects the strength of the Brønsted acid sites and product distribution. Mn and Zr have different catalytic functionalities. Mn oxides are known for their strong CO activation capabilities, while Zr oxides can effectively adsorb hydrogen via heterolytic or homolytic splitting. The combination of these functionalities provides complementary active sites for multiple reaction steps in the synthesis of light olefins. Mn oxides activate CO, while Zr oxides facilitate hydrogenation and hydrogen adsorption. Furthermore, the physical mixing of Mn and Zr components with the SAPO-34 zeolite creates a proximity effect, where the active sites of the two components are in close contact. This arrangement allows for more efficient transfer of reaction intermediates between the metal oxide and zeolite surfaces, thereby promoting desired reaction pathways [205].

Modification of mixed oxides with alkali metals increases the olefin/paraffin ratio and reduces hydrogenation activity [165]. On the other hand, copper (Cu), Zinc (Zn), and Cr-based catalysts are well-known to be active for methanol production from syngas. The composition and calcination temperature of CrZn mixed metal oxides play a significant role in determining their phase composition, crystallinity, and local coordination of Cr and Zn. Mixed metal oxides calcined at different temperatures exhibited different crystalline phases with varying Cr/Zn ratios, including ZnO, $ZnCr_2O_4$, and $ZnCrO_4$. The presence of different phases and changes in crystallinity were attributed to the temperature-dependent oxidation state of Cr and the formation of different chromates and spinels. The inversion degree of the $ZnCr_2O_4$ spinel structure was also found to be influenced by the Cr/Zn ratio and calcination temperature. Enrichment of the overall stability for olefin yield is achievable by a proliferation in the Cr/Zn ratio and a decline in calcination temperature [207]. On the other hand, the structure of SAPO-34 is one of the main parameters affecting catalyst performance and product selectivity. The nanosheet structure of selected SAPO-34 gives much higher CO conversion and light olefin selectivity than the regular one due to the large outer cages for the nanosheet structure of SAPO-34, which simplified the diffusion of reactants and products in the zeotype cages during the STO reaction over $ZnCrO_x$/SAPO-34 nanosheets [208].

$CO_2$ production during the syngas-to-light olefin process is a challenging issue that hinders the formation of the main product. Therefore, using a catalyst that minimizes $CO_2$ formation is one of the most critical challenges. The catalyst with a ZnZrO structure doped with Ce ($Zn_xCe_{2-y}Zr_yO_4$ over SAPO-34) enhances light olefin selectivity and CO conversion, while reducing methane selectivity. This is achieved by promoting surface oxygen vacancies and the presence of formate and methoxide species on the catalyst surface during direct synthesis gas transformation into lower olefins. These species are related to the activation and conversion of CO and $H_2$. $CH_3O^*$ species are identified as intermediates in the formation of light olefins. The introduction of cerium (Ce) enhances these processes, leading to improved catalytic performance. Furthermore, increasing the content of Ce/Zr only up to 2 shows a positive influence on light olefin selectivity. However, increasing it beyond two has a negative effect on product distribution. The role of SAPO-34 is vital in light olefin production because, without SAPO-34 support, methanol

is produced as the main product [209]. Adjusting the metal contents of catalysts further enhances catalytic activity, as observed with $Zn_{0.3}Ce_{1.0}Zr_1O_4$/SAPO-34 and $Zn_{0.5}CeZrO_x$/SAPO-34 composite catalysts using various complexing agents (citric acid, glucose, adipic acid, tartaric acid, and L-alanine). Among them, the bi-functional $Zn_{0.5}CeZrO_x$-glucose/SAPO-34 composite catalyst is supposed to give a much higher selectivity to light olefin, less methane selectivity, and high CO conversion. Surface oxygen vacancy is the main parameter that influences the direct transformation of syngas to light olefins. By increasing the surface oxygen vacancy of $Zn_{0.5}CeZrO_x$ by using glucose complexing agent, methanol intermediates production capacity, and in consequence, the production capacity of light olefins improves [210].

The decrease in CO conversion over times when using SAPO-18 as a support for the ZnCrOx catalyst is primarily due to its textural properties and significant acidity These factors contribute to the blockage of the SAPO-35 channels and coke formation, which initially promote methanol production but eventually lead to a rapid decline in CO conversion and light olefin selectivity. In contrast, SAPO-18 is preferred over SAPO-35 because it offers higher activity and stability, demonstrating better performance in maintaining CO conversion and light olefin selectivity during the reaction [211].

SAPO-17, is a member of SAPO zeolite family, stands out due to its unique framework structure and acid strength, distinguishing it from SAPO-18 and SAPO-34 zeolites. The specific topology of SAPO-17, characterized by weaker Brönsted acid sites and smaller pore openings, enhances its catalytic performance, particularly in the synthesis of light olefins like ethylene and propylene. These structural features not only promote higher selectivity towards ethylene and propylene but also reduce the formation of undesired paraffins. Consequently, SAPO-17 offers an improved catalytic performance compared to other traditional zeolites, making it a promising material for applications requiring high olefin selectivity [212].

The $MoS_2$/SAPO-34 catalyst offers a promising rout for CO conversion. However, its strong hydrogenation activity can lead to the formation of undesired products like methane and paraffins, limiting the selectivity towards the desired light olefins. However, when K is added to the catalyst, K weakens the hydrogenation ability of $MoS_2$, which is an advantage because it prevents excessive hydrogenation of olefins, allowing the formation of desired products like light olefins. All in all, zeolite provides additional catalytic sites and can promote coupling reactions that lead to the formation of $C_2$-$C_4$= olefins from $C_1$ intermediates. The presence of K weakens the hydrogenation ability of $MoS_2$, allowing more $C_1$ intermediates to undergo coupling reactions. This results in the production of light olefins instead of being solely hydrogenated to methane. This synergistic effect between $MoS_2$, K, and the zeolite leads to a more selective production of $C_2$-$C_4$= olefins with a higher olefin/paraffin ratio [213].

The preparation method of the catalyst is an effective parameter in the catalyst's properties and, specially, in its activity. In a research, $ZnZrO_x$ catalysts were prepared by calcinating Zn-UiO-66 (UiO-66 is an archetypal metal organic framework) in air and using traditional co-precipitation methods resulting in $ZnZrO_x$-400 and $ZnZrO_x$-P, respectively. These catalysts were used as bi-functional catalysts over SAPO-34 for light olefin synthesis from syngas. Catalysts were tested with an $H_2$/CO ratio of 2, temperature of 400°C, a pressure of 3 MPa, and a GHSV 3600 mL.g$^{-1}$.h$^{-1}$. The CO conversion of $ZnZrO_x$-400/SAPO-34 was almost twice as high as that of $ZnZrO_x$-P/SAPO-34. $ZnZrO_x$-400 exhibited a higher oxygen vacancy concentration, attributed to the smaller crystal size and the incorporation of more Zn into the $ZrO_2$ lattice. Due to its high temperature, which is conducive to MTO (methanol-to-olefins) reactions, SAPO-34 absorbs methanol and dimethyl ether (DME) produced over the oxides, accelerating the initial reaction step occurring on the oxide surfaces. The $ZnZrO_x$-400/SAPO-34 and $ZnZrO_x$-P/SAPO-34 bi-functional catalysts succeeded in achieving 79.7 % and 68.1 % selectivities for light olefins, respectively. The difference in selectivities could be attributed to the different hydrogenation abilities of $ZnZrO_x$ with different preparation methods [214]. As a result of the higher surface area and milder acidic properties of Fe@SAPO-34 catalyst, it has a higher tendency and ability to produce light olefins and limits the production of methane as the by-product compared to Fe and Fe/SAPO-34 catalysts [147].

Encapsulation is an advanced method of catalyst preparation, regarded as a new generation of bi-functional core@shell catalysts, where metallic oxide Zn-Cr is placed inside the zeolite SAPO-34 for the direct transformation of syngas to lower olefins. Methanol intermediates are produced in the Zn-Cr core, and the formation of light olefins occurs as the delivered methanol enters the acidic sites of SAPO-34. The formed $H_2O$ and light olefins are quickly removed in the catalyst after being formed by the suppression of side reactions. Higher methane selectivity and lower light olefin selectivity took place over the naked Zn-Cr catalyst, and when the reaction happens in two steps (Zn-Cr + SAPO-34), a slight increase in light olefin selectivity is obtained over the physical mixture of Zn-Cr/SAPO-34. The selectivity of light olefins considerably improves when the core@shell type is used [215].

The core@shell catalyst Fe/C@Si-SAPO not only increase the selectivity for light olefins but also reduces the selectivity for $C_{5+}$ hydrocarbons. This reduction is due to the core@shell structure, which allows the formed $C_{5+}$ hydrocarbons to escape from the SAPO-34 shell, facilitating their conversion into lighter ones. The core@shell structure is achieved by functionalizing the Fe/C particles with Si-OH groups, which influences the diffusion limitations and secondary reactions during the FTS process. However, a challenge with this catalyst is its higher methane production, attributed to the increased $H_2$/CO ratio within the core@shell structure. This ratio is influenced by the diffusion properties of $H_2$ and CO within the SAPO-34 shell. To address this issue, the addition of K as a promoter (Fe/C@Si-SAPO-K) has been shown to help suppress methane formation. K achieves this by inhibiting surface carbon hydrogenation and promoting carbon chain growth, thereby improving the overall selectivity toward light olefins [216].

The catalytic performance is closely linked to the structure of the shell. Different structures of silicalite-1 zeolite can be considered for mixed oxide catalysts for direct olefin production, including FeMnK oxide nanoparticles surrounded by the nanorod aggregated, hollow, and hollow mesoporous zeolite, indicated as FeMnK@S-1, FeMnK@Hol-S-1, and FeMnK@HM-S-1, respectively. Amonge these, FeMnK@HM-S-1 demonstrates the highest light olefins selectivity and CO conversion. This superior performance is attributed to its improved reactant diffusion and better access to active sites due to its higher surface area and more exposed active sites. Moreover, FeMnK@HM-S-1 exhibits a lower [H*]/[C*] ratio compared to other types, which favors the formation of olefins over methane. This ratio, representing the balance between chemisorbed hydrogen and carbon species on the catalyst surface, is crucial in determining product selectivity, with a lower ratio being more conducive to olefin production .[217].

In conclusion, recent advancements show that combining metal active phases with zeolite supports in bi-functional catalysts greatly enhances light olefin synthesis from syngas. Zeolites such as SAPO-34 and ZSM-5 are particularly effective, achieving olefin selectivities around 80 %. Modifying catalyst compositions and preparation methods can further improve performance. Despite challenges like $CO_2$ production and catalyst stability, zeolite-supported catalysts remain promising for efficient light olefin production, highlighting important directions for future research and industrial application.

### 3.3. Hybrid-supported catalysts

$Al_2O_3$ and zeolites, especially SAPO-34, are crucial supports, with Zn acting as the active phase and Zr as the promoter in hybrid catalysts for direct light olefin conversion. Fig. 12 schematically illustrates the difference between the performances of bi-functional catalysts and multi-step catalysts. In bi-functional catalysts, methanol production reaction occurs over metal sites, followed by light olefin production on the acidic
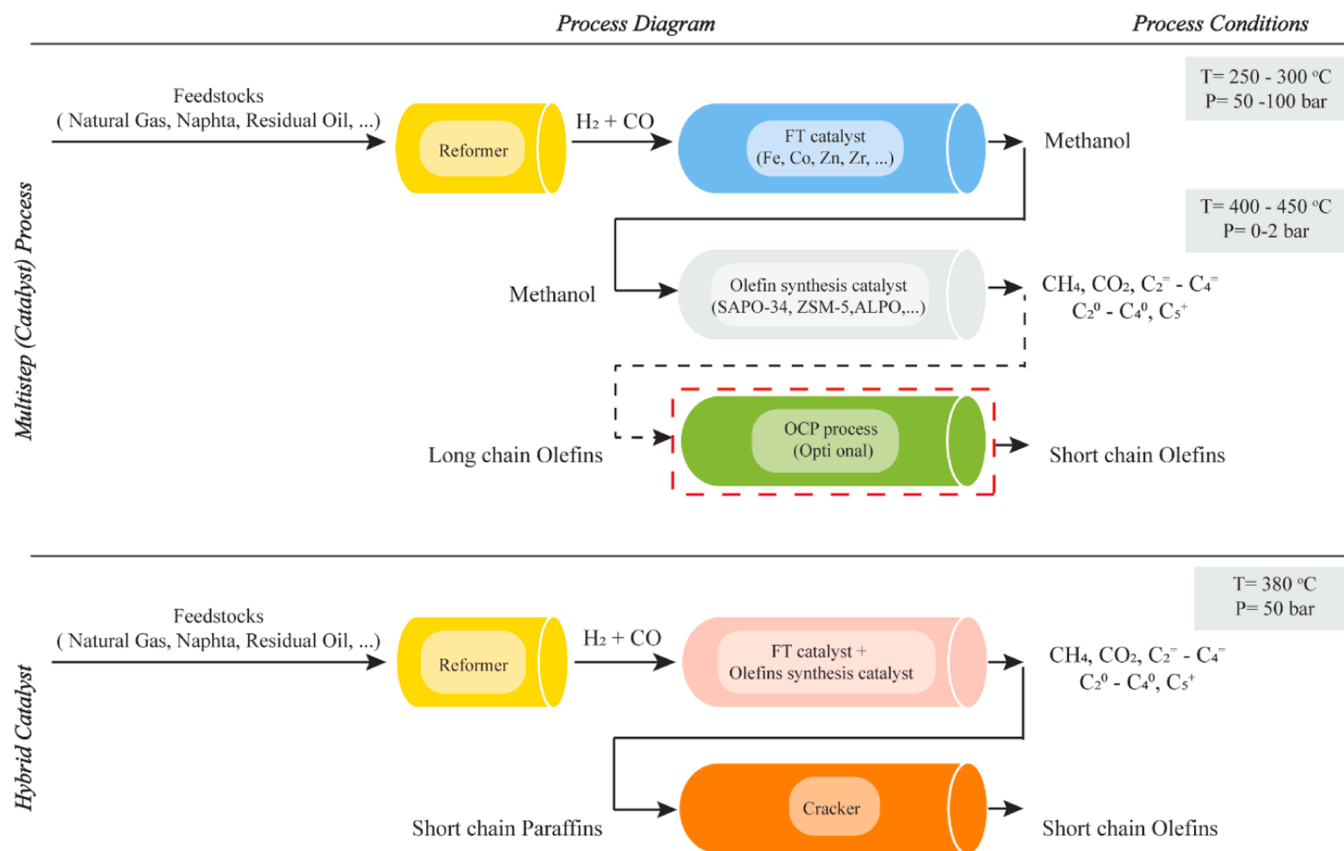
**Fig. 12.** Hybrid catalyst process concept [218].

sites of the support materials [137,144].

In a research, the role of doped Zr in a Zn/Al$_2$O$_3$-SAPO-34 catalyst and the effect of different weight ratios of Zn/Al$_2$O$_3$ with SAPO-34 were investigated. The research found that using 2 % Zr as a promoter in ZrZn/Al$_2$O$_3$-SAPO-34 showed remarkable light olefin selectivity and low methane selectivity. Doping Zr into ZnO causes structural modifications, potentially altering the surface properties and active sites of the catalyst. It also enhances the reduction temperature, suggesting that Zr incorporation improves the accessibility and reactivity of active sites due to the synergistic interaction between Zr-promoted Zn/Al$_2$O$_3$-SAPO-34 [219]. The presence of suitable acid and base properties, along with the co-existence of ZnO and spinel-structured ZnAl$_2$O$_4$, makes the La-doped Zn$_x$/Al$_y$O$_z$-SAPO-34 zeolite another effective hybrid catalyst. The pH values of precipitants significantly influence the formation of crystalline phases, which in turn affect the chemical composition, phase formation, porosity, and texture of catalysts, ultimately impacting their catalytic activity [220].

In conclusion, Al$_2$O$_3$ and SAPO-34 zeolite are essential supports for hybrid catalysts designed for direct light olefin conversion. Incoprating Zr into Zn/Al$_2$O$_3$-SAPO-34 enhances light olefin selectivity, while pH control during the preparation of La-doped Zn$_x$/Al$_y$O$_z$-SAPO-34 influences catalyst properties and catalytic activity. The light olefin, methane selectivity, and CO conversion, over bifunctional and hybrid supported catalysts are summarized in Fig. 13.

## 4. Conclusion and strategic approaches

The increasing demand for light olefins, coupled with the limitations of oil- derived feedstocks in the petrochemical industry, growing environmental concerns, and the depletion of non-renewable sources have driven the search for alternative production methods over the past decades. Traditionally, the catalytic SC process of hydrocarbons has been the primary source of light olefins, but this method is associated with high level of CO$_2$ emissions. Consequently, synthesis gas has emerged as a promising alternative for light olefin production sources. MTO and DMTO are key pathways for producing olefins from synthesis gas. These processes rely on specific catalysts and exhibit optimal performance in the presence of acidic zeolites, such as H-SAPO-34 and H-ZSM-5. Among these, DMTO processes are particularly favorable due to their thermodynamic characteristics and their potential to achieve high olefin yields and selectivity. Catalysts such as Ca-ZSM-5, La-ZSM-5, Ca-La-ZSM-5, La-Zr-ZSM-5, TiO$_2$-HZSM-5, HZSM-5/Al$_2$O$_3$, and SAPO-34 have shown significant promise in these reactions. Direct production of light olefins from syngas, known as the FTO process, effectively converts syngas to straight-chain hydrocarbons based on the ASF distribution. Optimizing this process involves modifying conventional FT catalysts by integrating FT-active metals with the acidic properties of zeolites, which are active in MTO and DMTO processes. This integration has demonstrated substantial potential for enhancing the indirect production of light olefins. In this review, we have systematically explored the intricacies of FT synthesis, focusing on both supported and unsupported catalysts, particularly those based on Fe and Co. Our findings highlight the distinctive characteristics and applications of these catalysts in FTO processes.

FTO catalysts can be categorized into three main types: conventional FT catalysts including unsupported and supported metal-based catalysts (with supports such as carbon, graphene, graphene oxide, zeolites, and metal oxides), bifunctional, and hybrid catalysts. Metals from Group IV-VI (e.g., Zr, Ti, Mo), Group XI-XII (e.g., Cu, Zn), and precious metals (e. g., Pt, Pd) favor dissociative CO adsorption but typically exhibit insufficient FTO activity. In contrast, Fe, and Co, are known to show significant FT activity.

Fe-based catalysts are noted for their high CO conversion rates and the production of a broad range of hydrocarbons but suffer from rapid
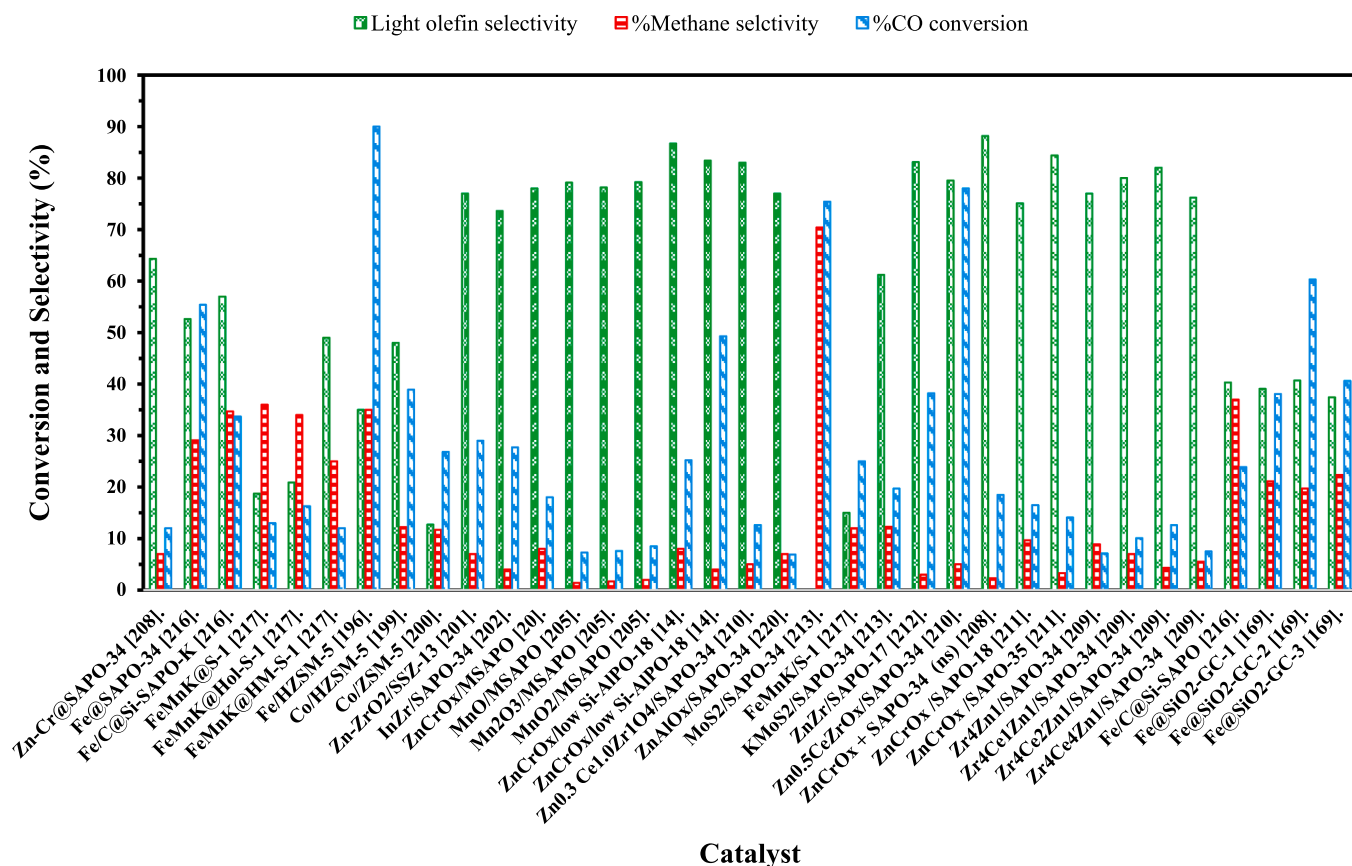
**Fig. 13.** Light olefin and methane selectivity, and CO conversion in bifunctional and hybrid supported catalysts.

deactivation. Co-based catalysts, while demonstrating high light olefin production and greater resistance to deactivation due to $H_2O$ production, necessitate a complex array of downstream operations. Enhancing FTO catalytic can be achieved through the use of promoters such as Na, Mg, K, Mn, Zn, V, Zr, and Cu oxides, which enhance CO adsorption and weaken the CO bond through electronic modulation.

The catalytic properties of unsupported catalysts are heavily influenced by the main element used. Group IV-VI metals, such as Zr, Ti, and Mo, promote dissociative CO adsorption but tend to form stable oxides, preventing the generation of active FT sites. Conversely, Group XI-XII metals and precious metals, despite their ability to dissociate CO, generally show poor activity for FTO conversion. Fe- and Co-based catalysts, particularly in their carbide forms, stand out for their significant activity in FT reactions, making them the most commonly used in the FTO process. The widely accepted mechanism for unsupported FTO catalysts involves a series of surface reactions that optimize the formation of light olefins (e.g., ethylene, propylene, butenes) from syngas. This process, known as the carbide mechanism, begins with the adsorption of CO and $H_2$ molecules onto the catalyst surface, where transition metals provide active sites for their dissociation. The subsequent formation of surface-bound $CH_3$ species and their reaction with additional CO and $H_2$ facilitate hydrocarbon chain growth, primarily forming surface carbides. Conditions favoring chain termination through beta-hydride elimination led to the release of light olefins, with their selectivity influenced by catalyst composition, promoters, reaction temperature, and pressure. Higher temperatures and lower pressures enhance olefin selectivity by favoring shorter hydrocarbon chains. Promoters play a crucial role in enhancing the performance of Fe and Co-based catalysts. For instance, alkali metals like Na and K improve CO adsorption and reduce methane selectivity, albeit sometimes at the cost of increased methane formation due to enhanced hydrogen chemisorption. Transition metals such as Mn and Zn increase olefin selectivity by

improving surface area and dissociative CO adsorption while reducing carbon deposition. Nonmetals like sulfur can enhance catalyst stability, although they need to be carefully controlled to avoid surface poisoning. The addition of structural promoters like Zn can significantly improve catalytic activity and light olefin selectivity by creating favorable surface chemistry and retarding secondary reactions.

Unsupported catalysts face significant challenges due to low mechanical stability and high carbon deposition. Therefore, porous supported catalysts are generally preferred due to their increased surface area, improved dispersion of the metal active phase, enhanced heat and mass transfer, and greater mechanical stability. Various supports, including $Al_2O_3$, $SiO_2$, CNT, and zeolites have been explored. Zeolites, in particular, are promising due to their acidic structure, which influences the adsorption and activation of CO molecules, the adsorption and dissociation of $H_2$ molecules over the active metal phase, the activation of CO and $H^*$, and the formation of methanol intermediates. Finally, the formed methanol converted to light olefins. The preparation methods of catalysts, such as impregnation, co-precipitation, sol-gel, and hydrothermal synthesis, are critical as they significantly impact the catalysts' physicochemical properties and performance. Additionally, post-synthesis treatments like calcination, reduction, and surface modifications play a crucial role in enhancing catalyst stability and reactivity.

To sum up, based on this paper, to effectively synthesize light olefins from syngas, a comprehensive understanding of catalyst performance and optimization is essential. This review highlights several strategic approaches to enhance the catalytic process, emphasizing the critical factors that influence catalyst selection and operation. Firstly, a thorough investigation into the advantages and limitations of using unsupported iron and cobalt catalysts in Fischer-Tropsch (FT) reactions is crucial. Specifically, focus should be placed on optimizing the chemical composition and synthesis techniques to enhance catalytic activity and selectivity for light olefins. Furthermore, the potential of various support

materials such as graphene oxide, carbon nanotubes, mixed metal oxides, and zeolites should be explored. Assessing how these supports influence the dispersion, stability, and reactivity of the active metal sites is vital.

Moreover, examining the emerging core@shell catalysts, which offer improved control over active site accessibility and stability, can provide insights into their performance in FT reactions and their potential to achieve high olefin selectivity. Additionally, the role of promoters such as Zn, Si, Ti, and Al in modifying the structural and electronic properties of the catalysts warrants detailed study. Therefore, understanding how these promoters influence CO conversion, olefin selectivity, and resistance to deactivation is essential.

Furthermore, investigating the formation of specific crystal phases and their impact on catalytic performance is important. Accordingly, highlighting the importance of maintaining well-defined active sites for enhanced reaction kinetics can further optimize the catalytic process. Moreover, evaluating the influence of reaction temperature and pressure on the activity and selectivity of the catalysts is critical. Thus, determining the optimal conditions that favor high olefin yield while minimizing undesirable by-products is necessary for efficient conversion. Additionally, analyzing the effect of syngas composition, including $H_2$/CO ratios, on catalyst performance can help identify the feedstock conditions that promote efficient conversion to light olefins. Also, reviewing various catalyst preparation methods, such as impregnation, co-precipitation, sol-gel, and hydrothermal synthesis, is essential to understand how these methods impact the physicochemical properties and performance of the catalysts. Additionally, considering the benefits of post-synthesis treatments like calcination, reduction, and surface modifications is important. Indeed, these treatments play a significant role in enhancing catalyst stability and reactivity.

Likewise, investigating common deactivation mechanisms, such as sintering, carbon deposition, and poisoning, is necessary to develop strategies to mitigate these issues and prolong catalyst life. Thus, exploring regeneration techniques to restore catalyst activity and maintain long-term performance is crucial. Furthermore, emphasizing the importance of developing robust and economically viable regeneration processes can ensure sustained catalytic efficiency.

Finally, focusing on the development of environmentally benign catalysts with reduced reliance on rare and expensive metals is critical for sustainable catalyst development. Additionally, implementing green synthesis methods and developing recyclable catalysts can contribute to sustainable industrial practices. Moreover, research should address the scalability of catalyst production, ensuring that high-performance catalysts can be manufactured cost-effectively for industrial applications. By adopting these strategic approaches, researchers can systematically address the challenges in syngas-to-olefins conversion. Ultimately, this review aims to provide a detailed understanding of the interplay between catalyst properties, reaction conditions, and performance, thereby guiding the development of highly efficient catalysts for light olefin production.

## CRediT authorship contribution statement

**Aligholi Niaei:** Writing – review & editing, Supervision. **Nagihan Delibas:** Writing – review & editing, Supervision. **Abdullah Zahid Turan:** Writing – review & editing, Supervision. **Gamze Behmenyar:** Writing – review & editing, Supervision. **Zahra Bahranifard:** Writing – review & editing. **Samira Farhoudi:** Writing – original draft, Methodology, Conceptualization. **Ali Sayyah:** Writing – original draft, Investigation, Conceptualization. **Elham Mahmoudi:** Writing – original draft, Methodology, Investigation, Conceptualization.

## Declaration of Competing Interest

The authors declare that they have no known competing financial interests or personal relationships that could have appeared to influence the work reported in this paper.

## Data availability

Data will be made available on request.

## Acknowledgments

## Appendix A. Supporting information

Supplementary data associated with this article can be found in the online version at doi:10.1016/j.jcou.2024.102893.

## References

[1] I. Amghizar, L.A. Vandewalle, K.M. Van Geem, G.B. Marin, New trends in olefin production, Engineering 3 (2017) 171–178.

[2] V. Sage, N. Burke, Use of probe molecules for Fischer–Tropsch mechanistic investigations: a short review, Catal. Today 178 (2011) 137–141.

[3] L. Zhong, F. Yu, Y. An, Y. Zhao, Y. Sun, Z. Li, T. Lin, Y. Lin, X. Qi, Y. Dai, Cobalt carbide nanoprisms for direct production of lower olefins from syngas, Nature 538 (2016) 84–87.

[4] X. Pan, F. Jiao, D. Miao, X. Bao, Oxide–zeolite-based composite catalyst concept that enables syngas chemistry beyond Fischer–Tropsch synthesis, Chem. Rev. 121 (2021) 6588–6609.

[5] T. Numpilai, C.K. Cheng, J. Limtrakul, T. Witoon, Recent advances in light olefins production from catalytic hydrogenation of carbon dioxide, Process Saf. Environ. Prot. 151 (2021) 401–427.

[6] H. Schmidbauer, A. Rösch, OPEC news announcements: effects on oil price expectation and volatility, Energy Econ. 34 (2012) 1656–1663.

[7] N. Kalantari, A. Farzi, F. Hamooni, N. Delibaş, A. Tarjomannejad, A. Niaei, D. Salari, Simultaneous study of different combinations of ZSM-5 templates and operating conditions in the MTP process; designing, modeling, and optimization by RSM-ANN-GA, J. Solgel Sci. Technol. (2024) 1–20.

[8] H.M. Torres Galvis, K.P. de Jong, Catalysts for production of lower olefins from synthesis gas: a review, ACS Catal. 3 (2013) 2130–2149.

[9] R. Davarnejad, Introductory Chapter: Olefins-Past, Now and Future, in: Alkenes-Recent Advances, New Perspectives and Applications, IntechOpen, 2021.

[10] S.A. Chernyak, M. Corda, J.-P. Dath, V.V. Ordomsky, A.Y. Khodakov, Light olefin synthesis from a diversity of renewable and fossil feedstocks: state-of the-art and outlook, Chem. Soc. Rev. 51 (2022) 7994–8044.

[11] M. Traver, A. Ebbinghaus, K. Moljord, K. Morganti, R. Pearson, M. Vermeire, Fuels and transportation, in: Energy Transition: Climate Action and Circularity, ACS Publications, 2022, pp. 83–129.

[12] A.D.N. Kamkeng, M. Wang, Technical analysis of the modified Fischer-Tropsch synthesis process for direct CO2 conversion into gasoline fuel: performance improvement via ex-situ water removal, Chem. Eng. J. 462 (2023) 142048.

[13] A. Al-Enazi, E.C. Okonkwo, Y. Bicer, T. Al-Ansari, A review of cleaner alternative fuels for maritime transportation, Energy Rep. 7 (2021) 1962–1985.

[14] J. Su, H. Zhou, S. Liu, C. Wang, W. Jiao, Y. Wang, C. Liu, Y. Ye, L. Zhang, Y. Zhao, Syngas to light olefins conversion with high olefin/paraffin ratio using ZnCrOx/AlPO-18 bifunctional catalysts, Nat. Commun. 10 (2019) 1297.

[15] S. Zhao, H. Li, B. Wang, X. Yang, Y. Peng, H. Du, Y. Zhang, D. Han, Z. Li, Recent advances on syngas conversion targeting light olefins, Fuel 321 (2022) 124124.

[16] M. Stöcker, Biofuels and biomass-to-liquid fuels in the biorefinery: catalytic conversion of lignocellulosic biomass using porous materials, Angew. Chem. Int. Ed. 47 (2008) 9200–9211.

[17] H.M.T. Galvis, J.H. Bitter, C.B. Khare, M. Ruitenbeek, A.I. Dugulan, K.P. de Jong, Supported iron nanoparticles as catalysts for sustainable production of lower olefins, Science (1979) 335 (2012) 835–838.

[18] K. Cheng, W. Zhou, J. Kang, S. He, S. Shi, Q. Zhang, Y. Pan, W. Wen, Y. Wang, Bifunctional catalysts for one-step conversion of syngas into aromatics with excellent selectivity and stability, Chem 3 (2017) 334–347.

[19] M. Oschatz, T.W. van Deelen, J.L. Weber, W.S. Lamme, G. Wang, B. Goderis, O. Verkinderen, A.I. Dugulan, K.P. De Jong, Effects of calcination and activation conditions on ordered mesoporous carbon supported iron catalysts for production of lower olefins from synthesis gas, Catal. Sci. Technol. 6 (2016) 8464–8473.

[20] F. Jiao, J. Li, X. Pan, J. Xiao, H. Li, H. Ma, M. Wei, Y. Pan, Z. Zhou, M. Li, Selective conversion of syngas to light olefins, Science 351 (2016) (1979) 1065–1068.

[21] T. Bhatelia, C. Li, Y. Sun, P. Hazewinkel, N. Burke, V. Sage, Chain length dependent olefin re-adsorption model for Fischer–Tropsch synthesis over Co-Al2O3 catalyst, Fuel Process. Technol. 125 (2014) 277–289.

[22] D. Wang, J. Ji, B. Chen, W. Chen, G. Qian, X. Duan, X. Zhou, A. Holmen, D. Chen, J.C. Walmsley, Novel Fe/MnK-CNTs nanocomposites as catalysts for direct production of lower olefins from syngas, AIChE J. 63 (2017) 154–161.

[23] C.G. Visconti, L. Lietti, P. Forzatti, R. Zennaro, Fischer–Tropsch synthesis on sulphur poisoned Co/Al2O3 catalyst, Appl. Catal. A Gen. 330 (2007) 49–56.

[24] P. Kaiser, R.B. Unde, C. Kern, A. Jess, Production of liquid hydrocarbons with CO2 as carbon source based on reverse water-gas shift and Fischer-Tropsch synthesis, Chem. Ing. Tech. 85 (2013) 489–499.

[25] A. Yahyazadeh, A.K. Dalai, W. Ma, L. Zhang, Fischer–Tropsch synthesis for light olefins from syngas: a review of catalyst development, Reactions 2 (2021) 227–257.

[26] C. Du, P. Lu, N. Tsubaki, Efficient and new production methods of chemicals and liquid fuels by carbon monoxide hydrogenation, ACS Omega 5 (2019) 49–56.

[27] S.-H. Kang, J.W. Bae, K.-J. Woo, P.S.S. Prasad, K.-W. Jun, ZSM-5 supported iron catalysts for Fischer–Tropsch production of light olefin, Fuel Process. Technol. 91 (2010) 399–403.

[28] F.G. Botes, The effect of a higher operating temperature on the Fischer–Tropsch/ HZSM-5 bifunctional process, Appl. Catal. A Gen. 284 (2005) 21–29.

[29] A. Usman, M.A.B. Siddiqui, A. Hussain, A. Aitani, S. Al-Khattaf, Catalytic cracking of crude oil to light olefins and naphtha: experimental and kinetic modeling, Chem. Eng. Res. Des. 120 (2017) 121–137.

[30] M. Arvidsson, P. Haro, M. Morandin, S. Harvey, Comparative thermodynamic analysis of biomass gasification-based light olefin production using methanol or DME as the platform chemical, Chem. Eng. Res. Des. 115 (2016) 182–194.

[31] D. Chen, K. Moljord, T. Fuglerud, A. Holmen, The effect of crystal size of SAPO-34 on the selectivity and deactivation of the MTO reaction, Microporous Mesoporous Mater. 29 (1999) 191–203.

[32] W. Xieqing, X. Chaogang, L. Zaiting, Z. Genquan, Catalytic processes for light olefin production, in: Practical Advances in Petroleum Processing, Springer, 2006, pp. 149–168.

[33] N. Rane, M. Kersbulck, R.A. Van Santen, E.J.M. Hensen, Cracking of n-heptane over Brønsted acid sites and Lewis acid Ga sites in ZSM-5 zeolite, Microporous Mesoporous Mater. 110 (2008) 279–291.

[34] T. Ren, M.K. Patel, K. Blok, Steam cracking and methane to olefins: Energy use, CO2 emissions and production costs, Energy 33 (2008) 817–833.

[35] S.P. Pyl, C.M. Schietekat, M.-F. Reyniers, R. Abhari, G.B. Marin, K.M.Van Geem, Biomass to olefins: cracking of renewable naphtha, Chem. Eng. J. 176 (2011) 178–187.

[36] D.W. Sauter, M. Taoufik, C. Boisson, Polyolefins, a success story, Polymers 9 (2017) 185.

[37] Z. Zhao, J. Jiang, F. Wang, An economic analysis of twenty light olefin production pathways, J. Energy Chem. 56 (2021) 193–202.

[38] Myer Kutz, Applied Plastics Engineering Handbook 1st Edition, 2011.

[39] T. Ren, M. Patel, K. Blok, Olefins from conventional and heavy feedstocks: energy use in steam cracking and alternative processes, Energy 31 (2006) 425–451.

[40] N. Rahimi, R. Karimzadeh, Catalytic cracking of hydrocarbons over modified ZSM-5 zeolites to produce light olefins: a review, Appl. Catal. A Gen. 398 (2011) 1–17.

[41] S.M. Jeong, J.H. Chae, W.-H. Lee, Study on the catalytic pyrolysis of naphtha over a KVO3/α-Al2O3 catalyst for production of light olefins, Ind. Eng. Chem. Res 40 (2001) 6081–6086.

[42] J.H. Song, P. Chen, S.H. Kim, G.A. Somorjai, R.J. Gartside, F.M. Dautzenberg, Catalytic cracking of n-hexane over MoO2, J. Mol. Catal. A Chem. 184 (2002) 197–202.

[43] H.K. Amusa, S. Adamu, I.A. Bakare, A.S. Arjah, S.A. Al-Bogami, S. Al-Ghamdi, S. A. Razzak, M.M. Hossain, High-performance VOx on SrO-γAl2O3 catalyst for oxidative cracking of n-hexane to light olefins under anaerobic environment, J. Ind. Eng. Chem. 89 (2020) 339–350.

[44] N. Kalantari, M.F. Bekheet, P.D.K. Nezhad, J.O. Back, A. Farzi, S. Penner, N. Delibaş, S. Schwarz, J. Bernardi, D. Salari, Effect of chromium and boron incorporation methods on structural and catalytic properties of hierarchical ZSM-5 in the methanol-to-propylene process, J. Ind. Eng. Chem. 111 (2022) 168–182.

[45] N. Kalantari, A. Farzi, N. Çaylak Delibaş, A. Niaei, D. Salari, Synthesis of multiple-template zeolites with various compositions and investigation of their catalytic properties, Res. Chem. Intermed. 47 (2021) 4957–4984.

[46] Y. Ji, H. Yang, W. Yan, Strategies to enhance the catalytic performance of ZSM-5 zeolite in hydrocarbon cracking: a review, Catalysts 7 (2017) 367.

[47] L. Xin, X. Liu, X. Chen, X. Feng, Y. Liu, C. Yang, Efficient conversion of light cycle oil into high-octane-number gasoline and light olefins over a mesoporous ZSM-5 catalyst, Energy Fuels 31 (2017) 6968–6976.

[48] S.M. Sadrameli, Thermal/catalytic cracking of liquid hydrocarbons for the production of olefins: A state-of-the-art review II: Catalytic cracking review, Fuel 173 (2016) 285–297.

[49] Y. Yoshimura, N. Kijima, T. Hayakawa, K. Murata, K. Suzuki, F. Mizukami, K. Matano, T. Konishi, T. Oikawa, M. Saito, Catalytic cracking of naphtha to light olefins, Catal. Surv. Jpn. 4 (2001) 157–167.

[50] D.J. Wilhelm, D.R. Simbeck, A.D. Karp, R.L. Dickenson, Syngas production for gas-to-liquids applications: technologies, issues and outlook, Fuel Process. Technol. 71 (2001) 139–148.

[51] J.R. Rostrup-Nielsen, New aspects of syngas production and use, Catal. Today 63 (2000) 159–164.

[52] A. Iulianelli, S. Liguori, J. Wilcox, A. Basile, Advances on methane steam reforming to produce hydrogen through membrane reactors technology: a review, Catal. Rev. 58 (2016) 1–35.

[53] K. Cheng, J. Kang, D.L. King, V. Subramanian, C. Zhou, Q. Zhang, Y. Wang, Advances in catalysis for syngas conversion to hydrocarbons, in: Advances in Catalysis, Elsevier, 2017, pp. 125–208.

[54] D. Chen, K. Moljord, A. Holmen, A methanol to olefins review: diffusion, coke formation and deactivation on SAPO type catalysts, Microporous Mesoporous Mater. 164 (2012) 239–250.

[55] W. Dai, X. Wang, G. Wu, N. Guan, M. Hunger, L. Li, Methanol-to-olefin conversion on silicoaluminophosphate catalysts: effect of Brønsted acid sites and framework structures, ACS Catal. 1 (2011) 292–299.

[56] M. Yang, D. Fan, Y. Wei, P. Tian, Z. Liu, Recent progress in methanol-to-olefins (MTO) catalysts, Adv. Mater. 31 (2019) 1902181.

[57] P. Tian, Y. Wei, M. Ye, Z. Liu, Methanol to olefins (MTO): from fundamentals to commercialization, ACS Catal. 5 (2015) 1922–1938.

[58] H.S. Kamaluddin, S.N. Basahel, K. Narasimharao, M. Mokhtar, H-ZSM-5 materials embedded in an amorphous silica matrix: highly selective catalysts for propylene in methanol-to-olefin process, Catalysts 9 (2019) 364.

[59] D. Chen, K. Moljord, T. Fuglerud, A. Holmen, The effect of crystal size of SAPO-34 on the selectivity and deactivation of the MTO reaction, Microporous Mesoporous Mater. 29 (1999) 191–203.

[60] J.Q. Chen, A. Bozzano, B. Glover, T. Fuglerud, S. Kvisle, Recent advancements in ethylene and propylene production using the UOP/Hydro MTO process, Catal. Today 106 (2005) 103–107.

[61] Y. Hong, V. Gruver, J.J. Fripiat, Role of Lewis Acidity in the Isomerization of n-Pentane and o-Xylene on Dealuminated H-Mordenites, J. Catal. 150 (1994) 421–429.

[62] Q. Sun, Y. Ma, N. Wang, X. Li, D. Xi, J. Xu, F. Deng, K.B. Yoon, P. Oleynikov, O. Terasaki, High performance nanosheet-like silicoaluminophosphate molecular sieves: synthesis, 3D EDT structural analysis and MTO catalytic studies, J. Mater. Chem. A Mater. 2 (2014) 17828–17839.

[63] I.M. Dahl, H. Mostad, D. Akporiaye, R. Wendelbo, Structural and chemical influences on the MTO reaction: a comparison of chabazite and SAPO-34 as MTO catalysts, Microporous Mesoporous Mater. 29 (1999) 185–190.

[64] Y. Lin, Y. Wei, L. Zhang, K. Guo, M. Wang, P. Huang, X. Meng, R. Zhang, Facile ionothermal synthesis of SAPO-LTA zeotypes with high structural stability and their catalytic performance in MTO reaction, Microporous Mesoporous Mater. 288 (2019) 109611.

[65] K. Hayat, X.-G. Li, W.-D. Xiao, Theoretical Insights into Intracrystalline Diffusion of Olefins in MTO Catalysts, Catal. Lett. 150 (2020) 2056–2067, https://doi.org/10.1007/s10562-020-03136-9.

[66] L. Xu, Z. Liu, A. Du, Y. Wei, Z. Sun, Synthesis, characterization, and MTO performance of MeAPSO-34 molecular sieves, in: Stud Surf Sci Catal, Elsevier, 2004, pp. 445–450.

[67] T. Weissenberger, B. Reiprich, A.G.F. Machoke, K. Klühspies, J. Bauer, R. Dotzel, J.L. Casci, W. Schwieger, Hierarchical MFI type zeolites with intracrystalline macropores: the effect of the macropore size on the deactivation behaviour in the MTO reaction, Catal. Sci. Technol. 9 (2019) 3259–3269.

[68] X. Bao, Y. Xu, Natural Gas Conversion VII: Proceedings of the 7th Natural Gas Conversion Symposium, Dalian, China, 6-10 June 2004, Elsevier, 2004.

[69] L.-T. Zhu, W.-Y. Ma, Z.-H. Luo, Influence of distributed pore size and porosity on MTO catalyst particle performance: Modeling and simulation, Chem. Eng. Res. Des. 137 (2018) 141–153.

[70] J. Zhong, J. Han, Y. Wei, S. Xu, Y. He, Y. Zheng, M. Ye, X. Guo, C. Song, Z. Liu, Increasing the selectivity to ethylene in the MTO reaction by enhancing diffusion limitation in the shell layer of SAPO-34 catalyst, Chem. Commun. 54 (2018) 3146–3149, https://doi.org/10.1039/C7CC09239C.

[71] M. Gao, H. Li, M. Yang, J. Zhou, X. Yuan, P. Tian, M. Ye, Z. Liu, A modeling study on reaction and diffusion in MTO process over SAPO-34 zeolites, Chem. Eng. J. 377 (2019) 119668, https://doi.org/10.1016/j.cej.2018.08.054.

[72] G. Cai, Z. Liu, R. Shi, H. Changqing, L. Yang, C. Sun, Y. Chang, Light alkenes from syngas via dimethyl ether, Appl. Catal. A Gen. 125 (1995) 29–38.

[73] N.V. Kolesnichenko, S.V. Konnov, V.S. Pavlov, O.V. Yashina, N.N. Ezhova, S. N. Khadzhiev, Dimethyl ether to olefins conversion in a slurry reactor: effects of the size of particles and the textural and acidic properties of the MFI-type zeolite, Pet. Chem. 57 (2017) 576–583.

[74] N.V. Kolesnichenko, O.V. Yashina, N.N. Ezhova, G.N. Bondarenko, S. N. Khadzhiev, Nanodispersed suspensions of zeolite catalysts for converting dimethyl ether into olefins, Russ. J. Phys. Chem. A 92 (2018) 113–123.

[75] S.N. Khadzhiev, N.V. Kolesnichenko, E.N. Khivrich, E.E. Kolesnikova, T.I. Batova, Stability of La-Zr-HZSM-5/Al 2 O 3 zeolite catalysts in the conversion of dimethyl ether to lower olefins, Pet. Chem. 53 (2013) 225–232.

[76] S.I. Abasov, F.A. Babayeva, B.B. Guliyev, N.N. Piriyev, M.I. Rustamov, Features of Methanol and Dimethyl Ether Conversion to Hydrocarbons on Modified Zeolites Y and ZSM-5, Theor. Exp. Chem. 49 (2013) 58–64, https://doi.org/10.1007/s11237-013-9295-9.

[77] N.V. Kolesnichenko, E.E. Kolesnikova, L.E. Kitaev, E.N. Biryukova, N. I. Trukhmanova, S.N. Khadzhiev, Zeolite catalysts modified with zirconium and sulfur compounds in the conversion of dimethyl ether to lower olefins, Pet. Chem. 52 (2012) 155–160.

[78] T. Kurniawan, O. Muraza, K. Miyake, A.S. Hakeem, Y. Hirota, A.M. Al-Amer, N. Nishiyama, Conversion of dimethyl ether to olefins over nanosized mordenite fabricated by a combined high-energy ball milling with recrystallization, Ind. Eng. Chem. Res 56 (2017) 4258–4266.

[79] G. Nasser, T. Kurniawan, K. Miyake, A. Galadima, Y. Hirota, N. Nishiyama, O. Muraza, Dimethyl ether to olefins over dealuminated mordenite (MOR) zeolites derived from natural minerals, J. Nat. Gas Sci. Eng. 28 (2016) 566–571.

[80] I.A. Bakare, O. Muraza, M.A. Sanhoob, K. Miyake, Y. Hirota, Z.H. Yamani, N. Nishiyama, Dimethyl ether-to-olefins over aluminum rich ZSM-5: The role of Ca and La as modifiers, Fuel 211 (2018) 18–26.

[81] T. Cordero-Lanzac, A.T. Aguayo, J. Bilbao, Reactor–regenerator system for the dimethyl ether-to-olefins process over HZSM-5 catalysts: conceptual development and analysis of the process variables, Ind. Eng. Chem. Res 59 (2020) 14689–14702.

[82] P. Pérez-Uriarte, A. Ateka, A.G. Gayubo, T. Cordero-Lanzac, A.T. Aguayo, J. Bilbao, Deactivation kinetics for the conversion of dimethyl ether to olefins over a HZSM-5 zeolite catalyst, Chem. Eng. J. 311 (2017) 367–377.

[83] T. Cordero-Lanzac, A. Ateka, P. Pérez-Uriarte, P. Castaño, A.T. Aguayo, J. Bilbao, Insight into the deactivation and regeneration of HZSM-5 zeolite catalysts in the conversion of dimethyl ether to olefins, Ind. Eng. Chem. Res 57 (2018) 13689–13702.

[84] A. Haas, C. Hauber, M. Kirchmann, Time-resolved product analysis of dimethyl ether-to-olefins conversion on SAPO-34, ACS Catal. 9 (2019) 5679–5691.

[85] M. Magomedova, E. Galanova, I. Davidov, M. Afokin, A. Maximov, Dimethyl ether to olefins over modified ZSM-5 based catalysts stabilized by hydrothermal treatment, Catalysts 9 (2019) 485.

[86] D. Zhao, Y. Zhang, Z. Li, Y. Wang, J. Yu, Synthesis of AEI/CHA intergrowth zeolites by dual templates and their catalytic performance for dimethyl ether to olefins, Chem. Eng. J. 323 (2017) 295–303.

[87] X. Zhang, L. Zhong, G. Zeng, Y. Gu, C. Peng, F. Yu, Z. Tang, Y. Sun, Process intensification of honeycomb fractal micro-reactor for the direct production of lower olefins from syngas, Chem. Eng. J. 351 (2018) 12–21.

[88] A. Corma, F.V. Melo, L. Sauvanaud, F. Ortega, Light cracked naphtha processing: controlling chemistry for maximum propylene production, Catal. Today 107-108 (2005) 699–706, https://doi.org/10.1016/j.cattod.2005.07.109.

[89] S. Wang, P. Wang, D. Shi, S. He, L. Zhang, W. Yan, Z. Qin, J. Li, M. Dong, J. Wang, Direct conversion of syngas into light olefins with low CO2 emission, ACS Catal. 10 (2020) 2046–2059.

[90] Z. Liu, C. Sun, G. Wang, Q. Wang, G. Cai, New progress in R&D of lower olefin synthesis, Fuel Process. Technol. 62 (2000) 161–172.

[91] H.M.T. Galvis, A.C.J. Koeken, J.H. Bitter, T. Davidian, M. Ruitenbeek, A. I. Dugulan, K.P. de Jong, Effects of sodium and sulfur on catalytic performance of supported iron catalysts for the Fischer–Tropsch synthesis of lower olefins, J. Catal. 303 (2013) 22–30.

[92] A. Keunecke, M. Dossow, V. Dieterich, H. Spliethoff, S. Fendt, Insights into Fischer–Tropsch catalysis: current perspectives, mechanisms, and emerging trends in energy research, Front Energy Res 12 (2024) 1344179.

[93] W.C.Q. Yu hl, T.J. Lin, W.Y.C. An yl, Q.Y. Chang, F. Yu, Y. Wei, F.F. Sun, Z. Jiang, S. Li SG, L.S. Zhong, Direct production of olefins from syngas with ultrahigh carbon efficiency [J], Nat. Commun. 13 (2022) 5987.

[94] S.A. Al-Sayari, Catalytic conversion of syngas to olefins over Mn–Fe catalysts, Ceram. Int 40 (2014) 723–728.

[95] J. Schneider, M. Struve, U. Trommler, M. Schlüter, L. Seidel, S. Dietrich, S. Rönsch, Performance of supported and unsupported Fe and Co catalysts for the direct synthesis of light alkenes from synthesis gas, Fuel Process. Technol. 170 (2018) 64–78.

[96] J.-B. Li, H.-F. Ma, H.-T. Zhang, Q.-W. Sun, W.-Y. Ying, D.-Y. Fang, Comparison of FeMn, FeMnNa and FeMnK catalysts for the preparation of light olefins from syngas, Acta Phys. -Chim. Sin. 30 (2014) 1932–1940.

[97] G.P. Van der Laan, A.A.C.M. Beenackers, Intrinsic kinetics of the gas–solid Fischer–Tropsch and water gas shift reactions over a precipitated iron catalyst, Appl. Catal. A Gen. 193 (2000) 39–53.

[98] B. Liu, W. Li, Y. Xu, Q. Lin, F. Jiang, X. Liu, Insight into the intrinsic active site for selective production of light olefins in cobalt-catalyzed Fischer–Tropsch Synthesis, ACS Catal. 9 (2019) 7073–7089.

[99] J. Van de Loosdrecht, F.G. Botes, I.M. Ciobica, A.C. Ferreira, P. Gibson, D. J. Moodley, A.M. Saib, J.L. Visagie, C.J. Weststrate, J.W. Niemantsverdriet, Fischer-Tropsch synthesis: catalysts and chemistry, in: Comprehensive Inorganic Chemistry II: From Elements to Applications, Elsevier, 2013, pp. 525–557.

[100] H. Mahmoudi, M. Mahmoudi, O. Doustdar, H. Jahangiri, A. Tsolakis, S. Gu, M. LechWyszynski, A review of Fischer Tropsch synthesis process, mechanism, surface chemistry and catalyst formulation, Biofuels Eng. 2 (2017) 11–31.

[101] M. Crocker, R. Andrews, The rationale for biofuels, Royal Society of Chemistry, Cambridge, UK, 2010.

[102] E. de Smit, B.M. Weckhuysen, The renaissance of iron-based Fischer–Tropsch synthesis: on the multifaceted catalyst deactivation behaviour, Chem. Soc. Rev. 37 (2008) 2758–2781, https://doi.org/10.1039/B805427D.

[103] X. Yang, J. Yang, Y. Wang, T. Zhao, H. Ben, X. Li, A. Holmen, Y. Huang, D. Chen, Promotional effects of sodium and sulfur on light olefins synthesis from syngas over iron-manganese catalyst, Appl. Catal. B 300 (2022) 120716.

[104] M. Zhang, J. Ren, Y. Yu, Insights into the hydrogen coverage effect and the mechanism of fischer–tropsch to olefins process on Fe5C2 (510), ACS Catal. 10 (2020) 689–701, https://doi.org/10.1021/acscatal.9b03639.

[105] Z. Gholami, F. Gholami, Z. Tišler, J. Hubáček, M. Tomas, M. Bačiak, M. Vakili, Production of light olefins via Fischer-Tropsch process using iron-based catalysts: a review, Catalysts 12 (2022) 174.

[106] H. Jahangiri, J. Bennett, P. Mahjoubi, K. Wilson, S. Gu, A review of advanced catalyst development for Fischer–Tropsch synthesis of hydrocarbons from biomass derived syn-gas, Catal. Sci. Technol. 4 (2014) 2210–2229, https://doi.org/10.1039/C4CY00327F.

[107] M. Al-Dossary, J.L.G. Fierro, J.J. Spivey, Cu-promoted Fe2O3/MgO-based Fischer–Tropsch catalysts of biomass-derived syngas, Ind. Eng. Chem. Res 54 (2015) 911–921.

[108] B. Chen, X. Zhang, W. Chen, D. Wang, N. Song, G. Qian, X. Duan, J. Yang, D. Chen, W. Yuan, Tailoring of Fe/MnK-CNTs composite catalysts for the Fischer–Tropsch synthesis of lower olefins from syngas, Ind. Eng. Chem. Res 57 (2018) 11554–11560.

[109] N. Chen, J. Zhang, Q. Ma, S. Fan, T.-S. Zhao, Hydrothermal preparation of Fe–Zr catalysts for the direct conversion of syngas to light olefins, RSC Adv. 6 (2016) 34204–34211.

[110] Z. Li, L. Zhong, F. Yu, Y. An, Y. Dai, Y. Yang, T. Lin, S. Li, H. Wang, P. Gao, Effects of sodium on the catalytic performance of CoMn catalysts for Fischer–Tropsch to olefin reactions, ACS Catal. 7 (2017) 3622–3631.

[111] Y. Liu, J.-F. Chen, J. Bao, Y. Zhang, Manganese-modified Fe3O4 microsphere catalyst with effective active phase of forming light olefins from syngas, ACS Catal. 5 (2015) 3905–3909.

[112] K.K. Ramasamy, M. Gray, H. Job, Y. Wang, Direct syngas hydrogenation over a Co–Ni bimetallic catalyst: process parameter optimization, Chem. Eng. Sci. 135 (2015) 266–273.

[113] G. Wang, K. Zhang, P. Liu, H. Hui, Y. Tan, Synthesis of light olefins from syngas over Fe–Mn–V–K catalysts in the slurry phase, J. Ind. Eng. Chem. 19 (2013) 961–965.

[114] V.V. Ordomsky, Y. Luo, B. Gu, A. Carvalho, P.A. Chernavskii, K. Cheng, A. Y. Khodakov, Soldering of iron catalysts for direct synthesis of light olefins from syngas under mild reaction conditions, ACS Catal. 7 (2017) 6445–6452.

[115] A. Masudi, N.W.C. Jusoh, O. Muraza, Opportunities for less-explored zeolitic materials in the syngas-to-olefins pathway over nanoarchitectured catalysts: a mini review, Catal. Sci. Technol. 10 (2020) 1582–1596.

[116] Z. Li, N. Yao, J. Cen, X. Li, L. Zhong, Y. Sun, M. He, Effects of alkali metal promoters on the structure–performance relationship of CoMn catalysts for Fischer–Tropsch synthesis, Catal. Sci. Technol. 10 (2020) 1816–1826.

[117] J.-B. Li, H.-F. Ma, H.-T. Zhang, Q.-W. Sun, W.-Y. Ying, D.-Y. Fang, Direct production of light olefins from syngas over potassium modified Fe–Mn catalyst, Reaction Kinetics, Mech. Catal. 112 (2014) 409–423.

[118] H. Zhang, H. Zhang, W. Qian, X. Wu, H. Ma, Q. Sun, W. Ying, Sodium modified Fe-Mn microsphere catalyst for Fischer–Tropsch synthesis of light olefins, Catal. Today (2020), https://doi.org/10.1016/j.cattod.2020.07.040.

[119] S. Yang, S. Lee, S.C. Kang, S.J. Han, K.-W. Jun, K.-Y. Lee, Y.T. Kim, Linear α-olefin production with Na-promoted Fe–Zn catalysts via Fischer–Tropsch synthesis, RSC Adv. 9 (2019) 14176–14187.

[120] P. Zhai, C. Xu, R. Gao, X. Liu, M. Li, W. Li, X. Fu, C. Jia, J. Xie, M. Zhao, X. Wang, Y.-W. Li, Q. Zhang, X.-D. Wen, D. Ma, Highly tunable selectivity for syngas-derived alkenes over zinc and sodium-modulated Fe5C2 catalyst, Angew. Chem. Int. Ed. 55 (2016) 9902–9907, https://doi.org/10.1002/anie.201603556.

[121] Z. Ma, W. Qian, H. Zhang, H. Ma, Q. Sun, W. Ying, High-temperature Fischer–Tropsch synthesis over the Li-promoted FeMnMgOx catalysts, Fuel 319 (2022) 123613.

[122] N. Lohitharn, J.G. Goodwin, Impact of Cr, Mn and Zr addition on Fe Fischer–Tropsch synthesis catalysis: investigation at the active site level using SSITKA, J. Catal. 257 (2008) 142–151, https://doi.org/10.1016/j.jcat.2008.04.015.

[123] X. Gao, J. Zhang, N. Chen, Q. Ma, S. Fan, T. Zhao, N. Tsubaki, Effects of zinc on Fe-based catalysts during the synthesis of light olefins from the Fischer-Tropsch process, Chin. J. Catal. 37 (2016) 510–516, https://doi.org/10.1016/S1872-2067(15)61051-8.

[124] F. Lu, J. Huang, Q. Wu, Y. Zhang, Mixture of α-Fe2O3 and MnO2 powders for direct conversion of syngas to light olefins, Appl. Catal. A Gen. 621 (2021) 118213.

[125] S. Zhang, D. Li, Y. Liu, Y. Zhang, Q. Wu, Zirconium doped precipitated Fe-based catalyst for Fischer–Tropsch synthesis to light olefins at industrially relevant conditions, Catal. Lett. 149 (2019) 1486–1495.

[126] Z. Ma, H. Ma, H. Zhang, X. Wu, W. Qian, Q. Sun, W. Ying, Direct conversion of syngas to light olefins through Fischer–Tropsch synthesis over Fe–Zr catalysts modified with sodium, ACS Omega 6 (2021) 4968–4976.

[127] J. Tu, M. Ding, Y. Zhang, Y. Li, T. Wang, L. Ma, C. Wang, X. Li, Synthesis of Fe3O4-nanocatalysts with different morphologies and its promotion on shifting C5+ hydrocarbons for Fischer–Tropsch synthesis, Catal. Commun. 59 (2015) 211–215.

[128] T. Lin, F. Yu, Y. An, T. Qin, L. Li, K. Gong, L. Zhong, Y. Sun, Cobalt carbide nanocatalysts for efficient syngas conversion to value-added chemicals with high selectivity, Acc. Chem. Res 54 (2021) 1961–1971.

[129] S. Liu, B. Sun, Y. Zhang, J. Li, D.E. Resasco, L. Nie, L. Wang, The role of intermediate Co x Mn 1− x O (x= 0.6–0.85) nanocrystals in the formation of active species for the direct production of lower olefins from syngas, Chem. Commun. 55 (2019) 6595–6598.

[130] Y. Dai, Y. Zhao, T. Lin, S. Li, F. Yu, Y. An, X. Wang, K. Xiao, F. Sun, Z. Jiang, Particle size effects of cobalt carbide for Fischer–Tropsch to olefins, ACS Catal. 9 (2018) 798–809.

[131] Y. An, T. Lin, F. Yu, X. Wang, Y. Lu, L. Zhong, H. Wang, Y. Sun, Effect of reaction pressures on structure–performance of Co2C-based catalyst for syngas conversion, Ind. Eng. Chem. Res 57 (2018) 15647–15653.

[132] J. Xie, P.P. Paalanen, T.W. van Deelen, B.M. Weckhuysen, M.J. Louwerse, K.P. de Jong, Promoted cobalt metal catalysts suitable for the production of lower olefins from natural gas, Nat. Commun. 10 (2019) 167.

[133] B. Wu, L. Bai, H. Xiang, Y.-W. Li, Z. Zhang, B. Zhong, An active iron catalyst containing sulfur for Fischer–Tropsch synthesis, Fuel 83 (2004) 205–212.

[134] Y. Yuan, S. Huang, H. Wang, Y. Wang, J. Wang, J. Lv, Z. Li, X. Ma, Monodisperse Nano-Fe3O4 on α-Al2O3 Catalysts for Fischer–Tropsch Synthesis to Lower Olefins: promoter and size effects, ChemCatChem 9 (2017) 3144–3152.

[135] M. Zhao, C. Yan, S. Jinchang, Z. Qianwen, Modified iron catalyst for direct synthesis of light olefin from syngas, Catal. Today 316 (2018) 142–148.

[136] J.-B. Li, H.-F. Ma, H.-T. Zhang, Q.-W. Sun, W.-Y. Ying, D.-Y. Fang, Sodium promoter on iron-based catalyst for direct catalytic synthesis of light alkenes from syngas, Fuel Process. Technol. 125 (2014) 119–124, https://doi.org/10.1016/j.fuproc.2014.03.017.

[137] Y. Zhou, S. Natesakhawat, T. Nguyen-Phan, D.R. Kauffman, C.M. Marin, K. Kisslinger, R. Lin, H.L. Xin, E. Stavitski, K. Attenkofer, Highly active and stable carbon nanosheets supported iron oxide for Fischer-Tropsch to olefins synthesis, ChemCatChem 11 (2019) 1625–1632.

[138] J. Chai, J. Jiang, Y. Gong, P. Wu, A. Wang, X. Zhang, T. Wang, X. Meng, Q. Lin, Y. Lv, Recent mechanistic understanding of fischer-tropsch synthesis on Fe-carbide, Catalysts 13 (2023) 1052.

[139] K. Yuan, X.-C. Sun, H.-J. Yin, L. Zhou, H.-C. Liu, C.-H. Yan, Y.-W. Zhang, Boosting the water gas shift reaction on Pt/CeO2-based nanocatalysts by compositional modification: support doping versus bimetallic alloying, J. Energy Chem. 67 (2022) 241–249.

[140] Q. Zhang, J. Kang, Y. Wang, Development of novel catalysts for Fischer–Tropsch synthesis: tuning the product selectivity, ChemCatChem 2 (2010) 1030–1058.

[141] H. Chen, F. Goodarzi, Y. Mu, S. Chansai, J.J. Mielby, B. Mao, T. Sooknoi, C. Hardacre, S. Kegnæs, X. Fan, Effect of metal dispersion and support structure of Ni/silicalite-1 catalysts on non-thermal plasma (NTP) activated CO2 hydrogenation, Appl. Catal. B 272 (2020) 119013.

[142] H. Yi, Q. Xue, S. Lu, J. Wu, Y. Wang, G. Luo, Effect of pore structure on Ni/Al2O3 microsphere catalysts for enhanced CO2 methanation, Fuel 315 (2022) 123262.

[143] R. Munirathinam, D. Pham Minh, A. Nzihou, Effect of the support and its surface modifications in cobalt-based Fischer–Tropsch synthesis, Ind. Eng. Chem. Res 57 (2018) 16137–16161.

[144] M. Rahmati, B. Huang, M.K. Mortensen, K. Keyvanloo, T.H. Fletcher, B. F. Woodfield, W.C. Hecker, M.D. Argyle, Effect of different alumina supports on performance of cobalt Fischer-Tropsch catalysts, J. Catal. 359 (2018) 92–100, https://doi.org/10.1016/j.jcat.2017.12.022.

[145] I.M. Dahl, S. Kolboe, On the reaction mechanism for hydrocarbon formation from methanol over SAPO-34: I. Isotopic labeling studies of the co-reaction of ethene and methanol, J. Catal. 149 (1994) 458–464.

[146] B. Sun, G. Yu, J. Lin, K. Xu, Y. Pei, S. Yan, M. Qiao, K. Fan, X. Zhang, B. Zong, A highly selective Raney Fe@ HZSM-5 Fischer–Tropsch synthesis catalyst for gasoline production: one-pot synthesis and unexpected effect of zeolites, Catal. Sci. Technol. 2 (2012) 1625–1629.

[147] Z. Di, T. Zhao, X. Feng, M. Luo, A newly designed core-shell-like zeolite capsule catalyst for synthesis of light olefins from syngas via Fischer–Tropsch synthesis reaction, Catal. Lett. 149 (2019) 441–448.

[148] S. Mohammadnasabomran, A. Tavasoli, Y. Zamani, The impact of different alumina supports on cobalt-catalyzed Fischer–Tropsch synthesis and investigation of kinetic model for the catalyst with optimum performance, React. Kinet., Mech. Catal. 128 (2019) 217–234.

[149] X. Li, M.U. Nisa, Y. Chen, Z. Li, Co-based catalysts supported on silica and carbon materials: effect of support property on cobalt species and Fischer–Tropsch synthesis performance, Ind. Eng. Chem. Res 58 (2019) 3459–3467.

[150] K. Shimura, T. Miyazawa, T. Hanaoka, S. Hirata, Fischer–Tropsch synthesis over alumina supported cobalt catalyst: Effect of promoter addition, Appl. Catal. A Gen. 494 (2015) 1–11, https://doi.org/10.1016/j.apcata.2015.01.017.

[151] K. Jalama, N.J. Coville, H. Xiong, D. Hildebrandt, D. Glasser, S. Taylor, A. Carley, J.A. Anderson, G.J. Hutchings, A comparison of Au/Co/Al2O3 and Au/Co/SiO2 catalysts in the Fischer–Tropsch reaction, Appl. Catal. A Gen. 395 (2011) 1–9.

[152] G.L. Bezemer, J.H. Bitter, H.P.C.E. Kuipers, H. Oosterbeek, J.E. Holewijn, X. Xu, F. Kapteijn, A.J. van Dillen, K.P. de Jong, Cobalt particle size effects in the fischer–tropsch reaction studied with carbon nanofiber supported catalysts, J. Am. Chem. Soc. 128 (2006) 3956–3964, https://doi.org/10.1021/ja058282w.

[153] M. Zhao, J. Sun, X. Li, Q. Zhang, Synthesis of light olefins from syngas catalyzed by supported iron-based catalysts on alumina, Catal. Today 402 (2022) 300–309.

[154] Z.-Q. Huang, T.-H. Li, B. Yang, C.-R. Chang, Role of surface frustrated Lewis pairs on reduced CeO2(110) in direct conversion of syngas, Chin. J. Catal. 41 (2020) 1906–1915, https://doi.org/10.1016/S1872-2067(20)63627-0.

[155] Z. Zhang, W. Dai, X.-C. Xu, J. Zhang, B. Shi, J. Xu, W. Tu, Y.-F. Han, MnOx promotional effects on olefins synthesis directly from syngas over bimetallic Fe-MnOx/SiO2 catalysts, AIChE J. 63 (2017) 4451–4464, https://doi.org/10.1002/aic.15796.

[156] R. Zafari, M. Abdouss, Y. Zamani, A. Tavasoli, An efficient catalyst for light olefins production from CO hydrogenation: synergistic effect of Zn and Ce promoters on performance of Co–Mn/SiO2 Catalyst, Catal. Lett. 147 (2017) 2475–2486, https://doi.org/10.1007/s10562-017-2152-z.

[157] H. Zohdi-Fasaei, H. Atashi, F.F. Tabrizi, A.A. Mirzaei, Exploiting the effects of catalyst geometric properties to boost the formation of light olefins in Fischer-Tropsch synthesis: statistical approach for simultaneous optimization, J. Nat. Gas. Sci. Eng. 35 (2016) 1025–1031.

[158] Y. Liu, F. Lu, Y. Tang, M. Liu, F.F. Tao, Y. Zhang, Effects of initial crystal structure of Fe2O3 and Mn promoter on effective active phase for syngas to light olefins, Appl. Catal. B 261 (2020) 118219.

[159] S. Guo, Q. Wang, M. Wang, Z. Ma, J. Wang, B. Hou, C. Chen, M. Xia, L. Jia, D. Li, A comprehensive insight into the role of barium in catalytic performance of Co/Al2O3 catalyst for Fischer-Tropsch synthesis, Fuel 256 (2019) 115911.

[160] N.H. Jabarullah, Production of olefins from syngas over Al2O3 supported Ni and Cu nano-catalysts, Pet. Sci. Technol. 37 (2019) 382–385.

[161] I.K. Ghosh, Z. Iqbal, T. van Heerden, E. van Steen, A. Bordoloi, Insights into the unusual role of chlorine in product selectivity for direct hydrogenation of CO/CO2 to short-chain olefins, Chem. Eng. J. 413 (2021) 127424.

[162] H. Zhang, H. Ma, H. Zhang, W. Ying, D. Fang, Effects of Zr and K promoters on precipitated iron-based catalysts for Fischer–Tropsch synthesis, Catal. Lett. 142 (2012) 131–137.

[163] Y. An, T. Lin, F. Yu, Y. Yang, L. Zhong, M. Wu, Y. Sun, Advances in direct production of value-added chemicals via syngas conversion, Sci. China Chem. 60 (2017) 887–903.

[164] X. Wang, W. Chen, T. Lin, J. Li, F. Yu, Y. An, Y. Dai, H. Wang, L. Zhong, Y. Sun, Effect of the support on cobalt carbide catalysts for sustainable production of olefins from syngas, Chin. J. Catal. 39 (2018) 1869–1880.

[165] S. Saheli, A.R. Rezvani, A. Arabshahi, M. Dusek, E. Samolova, M. Jarosova, Synthesis new Co–Mn mixed oxide catalyst for the production of light olefins by tuning the catalyst structure, Appl. Organomet Chem. 35 (2021) e6038.

[166] J.-D. Xu, Z.-Y. Chang, K.-T. Zhu, X.-F. Weng, W.-Z. Weng, Y.-P. Zheng, C.-J. Huang, H.-L. Wan, Effect of sulfur on α-Al2O3-supported iron catalyst for Fischer–Tropsch synthesis, Appl. Catal. A Gen. 514 (2016) 103–113.

[167] M. Akbari, A.A. Mirzaei, M. Arsalanfar, Microemulsion based synthesis of promoted Fe–Co/MgO nanocatalyst: influence of calcination atmosphere on the physicochemical properties, activity and light olefins selectivity for hydrogenation of carbon monoxide, Mater. Chem. Phys. 249 (2020) 123003.

[168] Y. Xu, J. Wang, G. Ma, J. Bai, Y. Du, M. Ding, Selective conversion of syngas to olefins-rich liquid fuels over core-shell FeMn@SiO2 catalysts, Fuel 275 (2020) 117884, https://doi.org/10.1016/j.fuel.2020.117884.

[169] Z. Ni, H. Qin, S. Kang, J. Bai, Z. Wang, Y. Li, Z. Zheng, X. Li, Effect of graphitic carbon modification on the catalytic performance of Fe@SiO2-GC catalysts for forming lower olefins via Fischer-Tropsch synthesis, J. Colloid Interface Sci. 516 (2018) 16–22, https://doi.org/10.1016/j.jcis.2018.01.017.

[170] W. Chen, Z. Fan, X. Pan, X. Bao, Effect of confinement in carbon nanotubes on the activity of fischer−tropsch iron catalyst, J. Am. Chem. Soc. 130 (2008) 9414–9419, https://doi.org/10.1021/ja8008192.

[171] H.J. Schulte, B. Graf, W. Xia, M. Muhler, Nitrogen-and oxygen-functionalized multiwalled carbon nanotubes used as support in iron-catalyzed, high-temperature fischer–tropsch synthesis, ChemCatChem 4 (2012) 350–355.

[172] J. Lu, L. Yang, B. Xu, Q. Wu, D. Zhang, S. Yuan, Y. Zhai, X. Wang, Y. Fan, Z. Hu, Promotion effects of nitrogen doping into carbon nanotubes on supported iron Fischer–Tropsch catalysts for lower olefins, ACS Catal. 4 (2014) 613–621.

[173] Z. Zhang, J. Zhang, X. Wang, R. Si, J. Xu, Y.-F. Han, Promotional effects of multiwalled carbon nanotubes on iron catalysts for Fischer-Tropsch to olefins, J. Catal. 365 (2018) 71–85.

[174] B. Gu, V.V. Ordomsky, M. Bahri, O. Ersen, P.A. Chernavskii, D. Filimonov, A. Y. Khodakov, Effects of the promotion with bismuth and lead on direct synthesis of light olefins from syngas over carbon nanotube supported iron catalysts, Appl. Catal. B 234 (2018) 153–166.

[175] Z. Yang, X. Pan, J. Wang, X. Bao, FeN particles confined inside CNT for light olefin synthesis from syngas: Effects of Mn and K additives, Catal. Today 186 (2012) 121–127.

[176] B. Gu, C. Zhou, S. He, S. Moldovan, P.A. Chernavskii, V.V. Ordomsky, A. Y. Khodakov, Size and promoter effects on iron nanoparticles confined in carbon nanotubes and their catalytic performance in light olefin synthesis from syngas, Catal. Today 357 (2020) 203–213.

[177] B. Gu, S. He, D.V. Peron, D.R.S. Pedrolo, S. Moldovan, M.C. Ribeiro, B. Lobato, P. A. Chernavskii, V.V. Ordomsky, A.Y. Khodakov, Synergy of nanoconfinement and promotion in the design of efficient supported iron catalysts for direct olefin synthesis from syngas, J. Catal. 376 (2019) 1–16.

[178] B. Gu, D.V. Peron, A.J. Barrios, M. Bahri, O. Ersen, M. Vorokhta, B. Šmíd, D. Banerjee, M. Virginie, E. Marceau, Mobility and versatility of the liquid bismuth promoter in the working iron catalysts for light olefin synthesis from syngas, Chem. Sci. 11 (2020) 6167–6182.

[179] J. Xie, H.M. Torres Galvis, A.C.J. Koeken, A. Kirilin, A.I. Dugulan, M. Ruitenbeek, K.P.De Jong, Size and promoter effects on stability of carbon-nanofiber-supported iron-based Fischer–Tropsch catalysts, ACS Catal. 6 (2016) 4017–4024.

[180] K. Asami, A. Iwasa, N. Igarashi, S. Takemiya, K. Yamamoto, K. Fujimoto, Fischer–Tropsch synthesis over precipitated iron catalysts supported on carbon, Catal. Today 215 (2013) 80–85.

[181] K. Asami, K. Komiyama, K. Yoshida, H. Miyahara, Synthesis of lower olefins from synthesis gas over active carbon-supported iron catalyst, Catal. Today 303 (2018) 117–122.

[182] Z. Tian, C. Wang, Z. Si, L. Ma, L. Chen, Q. Liu, Q. Zhang, H. Huang, Fischer-Tropsch synthesis to light olefins over iron-based catalysts supported on KMnO4 modified activated carbon by a facile method, Appl. Catal. A Gen. 541 (2017) 50–59.

[183] H. Xiong, M.A. Motchelaho, M. Moyo, L.L. Jewell, N.J. Coville, Effect of Group I alkali metal promoters on Fe/CNT catalysts in Fischer–Tropsch synthesis, Fuel 150 (2015) 687–696.

[184] X. Chen, D. Deng, X. Pan, Y. Hu, X. Bao, N-doped graphene as an electron donor of iron catalysts for CO hydrogenation to light olefins, Chem. Commun. 51 (2015) 217–220.

[185] S.O. Moussa, L.S. Panchakarla, M.Q. Ho, M.S. El-Shall, Graphene-supported, iron-based nanoparticles for catalytic production of liquid hydrocarbons from synthesis gas: the role of the graphene support in comparison with carbon nanotubes, ACS Catal. 4 (2014) 535–545.

[186] A.-H. Nasser, L. Guo, H. ELnaggar, Y. Wang, X. Guo, A. AbdelMoneim, N. Tsubaki, Mn–Fe nanoparticles on a reduced graphene oxide catalyst for enhanced olefin production from syngas in a slurry reactor, RSC Adv. 8 (2018) 14854–14863.

[187] R. Zafari, M. Abdouss, Y. Zamani, Effect of Mn and reduced graphene oxide for the Fischer–Tropsch reaction: an efficient catalyst for the production of light olefins from syngas, React. Kinet., Mech. Catal. 129 (2020) 707–724.

[188] Z. Tian, C. Wang, J. Yue, X. Zhang, L. Ma, Effect of a potassium promoter on the Fischer–Tropsch synthesis of light olefins over iron carbide catalysts encapsulated in graphene-like carbon, Catal. Sci. Technol. 9 (2019) 2728–2741.

[189] C.C. Amoo, C. Xing, N. Tsubaki, J. Sun, Tandem reactions over zeolite-based catalysts in syngas conversion, ACS Cent. Sci. 8 (2022) 1047–1062.

[190] M. Moliner, C. Martinez, A. Corma, Synthesis strategies for preparing useful small pore zeolites and zeotypes for gas separations and catalysis, Chem. Mater. 26 (2014) 246–258.

[191] H.T. Luk, C. Mondelli, S. Mitchell, D.C. Ferré, J.A. Stewart, J. Pérez–Ramírez, Impact of carrier acidity on the conversion of syngas to higher alcohols over zeolite-supported copper-iron catalysts, J. Catal. 371 (2019) 116–125.

[192] W. Zhou, K. Cheng, J. Kang, C. Zhou, V. Subramanian, Q. Zhang, Y. Wang, New horizon in C1 chemistry: breaking the selectivity limitation in transformation of syngas and hydrogenation of CO2 into hydrocarbon chemicals and fuels, Chem. Soc. Rev. 48 (2019) 3193–3228, https://doi.org/10.1039/C8CS00502H.

[193] S. Sartipi, M. Alberts, M.J. Meijerink, T.C. Keller, J. Pérez-Ramírez, J. Gascon, F. Kapteijn, Towards liquid fuels from biosyngas: effect of zeolite structure in hierarchical-zeolite-supported cobalt catalysts, ChemSusChem 6 (2013) 1646–1650.

[194] R. Bai, Y. Song, Y. Li, J. Yu, Creating hierarchical pores in zeolite catalysts, Trends Chem. 1 (2019) 601–611.

[195] K.P. de Jong, Surprised by selectivity, Science 351 (2016) (1979) 1030–1031.

[196] J.L. Weber, I. Dugulan, P.E. de Jongh, K.P.De Jong, Bifunctional catalysis for the conversion of synthesis gas to olefins and aromatics, ChemCatChem 10 (2018) 1107–1112.

[197] Y. Xu, J. Liu, G. Ma, J. Wang, J. Lin, H. Wang, C. Zhang, M. Ding, Effect of iron loading on acidity and performance of Fe/HZSM-5 catalyst for direct synthesis of aromatics from syngas, Fuel 228 (2018) 1–9.

[198] J.L. Weber, N.A. Krans, J.P. Hofmann, E.J.M. Hensen, J. Zecevic, P.E. De Jongh, K.P. De Jong, Effect of proximity and support material on deactivation of bifunctional catalysts for the conversion of synthesis gas to olefins and aromatics, Catal. Today 342 (2020) 161–166.

[199] B. Maddi, S. Davidson, H. Job, R. Dagle, M. Guo, M. Gray, K.K. Ramasamy, Production of gaseous olefins from syngas over a cobalt-HZSM-5 catalyst, Catal. Lett. 151 (2021) 526–537.

[200] V. Subramanian, V.L. Zholobenko, K. Cheng, C. Lancelot, S. Heyte, J. Thuriot, S. Paul, V.V. Ordomsky, A.Y. Khodakov, The role of steric effects and acidity in the direct synthesis of iso-paraffins from syngas on cobalt zeolite catalysts, ChemCatChem 8 (2016) 380–389.

[201] X. Liu, W. Zhou, Y. Yang, K. Cheng, J. Kang, L. Zhang, G. Zhang, X. Min, Q. Zhang, Y. Wang, Design of efficient bifunctional catalysts for direct conversion of syngas into lower olefins via methanol/dimethyl ether intermediates, Chem. Sci. 9 (2018) 4708–4718.

[202] J. Su, D. Wang, Y. Wang, H. Zhou, C. Liu, S. Liu, C. Wang, W. Yang, Z. Xie, M. He, Direct Conversion of Syngas into Light Olefins over Zirconium-Doped Indium (III) Oxide and SAPO-34 Bifunctional Catalysts: Design of Oxide Component and Construction of Reaction Network, ChemCatChem 10 (2018) 1536–1541.

[203] G. Li, F. Jiao, X. Pan, N. Li, D. Miao, L. Li, X. Bao, Role of SAPO-18 acidity in direct syngas conversion to light olefins, ACS Catal. 10 (2020) 12370–12375.

[204] K. Cheng, B. Gu, X. Liu, J. Kang, Q. Zhang, Y. Wang, Direct and highly selective conversion of synthesis gas into lower olefins: design of a bifunctional catalyst combining methanol synthesis and carbon–carbon coupling, Angew. Chem. Int. Ed. 55 (2016) 4725–4728.

[205] C. Du, L.G. Chizema, E. Hondo, M. Tong, Q. Ma, X. Gao, R. Yang, P. Lu, N. Tsubaki, One-step conversion of syngas to light olefins over bifunctional metal-zeolite catalyst, Chin. J. Chem. Eng. 36 (2021) 101–110.

[206] Y. Zhu, X. Pan, F. Jiao, J. Li, J. Yang, M. Ding, Y. Han, Z. Liu, X. Bao, Role of manganese oxide in syngas conversion to light olefins, ACS Catal. 7 (2017) 2800–2804.

[207] V.P. Santos, G. Pollefeyt, D.F. Yancey, A.C. Sandikci, B. Vanchura, D.L. S. Nieskens, M. de Kok-Kleiberg, A. Kirilin, A. Chojecki, A. Malek, Direct conversion of syngas to light olefins (C2–C3) over a tandem catalyst CrZn–SAPO-34: tailoring activity and stability by varying the Cr/Zn ratio and calcination temperature, J. Catal. 381 (2020) 108–120.

[208] Y. Huang, H. Ma, Z. Xu, W. Qian, H. Zhang, W. Ying, Role of nanosized sheet-like SAPO-34 in bifunctional catalyst for syngas-to-olefins reaction, Fuel 273 (2020) 117771.

[209] F. Meng, X. Li, P. Zhang, L. Yang, G. Yang, P. Ma, Z. Li, Highly active ternary oxide ZrCeZnOx combined with SAPO-34 zeolite for direct conversion of syngas into light olefins, Catal. Today 368 (2021) 118–125.

[210] Y. Luo, S. Wang, S. Guo, K. Yuan, H. Wang, M. Dong, Z. Qin, W. Fan, J. Wang, Conversion of syngas into light olefins over bifunctional ZnCeZrO/SAPO-34 catalysts: regulation of the surface oxygen vacancy concentration and its relation to the catalytic performance, Catal. Sci. Technol. 11 (2021) 338–348.

[211] Y. Huang, H. Ma, Z. Xu, W. Qian, H. Zhang, W. Ying, Utilization of SAPO-18 or SAPO-35 in the bifunctional catalyst for the direct conversion of syngas to light olefins, RSC Adv. 11 (2021) 13876–13884.

[212] J. Su, C. Liu, S. Liu, Y. Ye, Y. Du, H. Zhou, S. Liu, W. Jiao, L. Zhang, C. Wang, High conversion of syngas to ethene and propene on bifunctional catalysts via the tailoring of SAPO zeolite structure, Cell Rep. Phys. Sci. 2 (2021).

[213] H. Zhou, S. Liu, J. Su, C. Liu, L. Zhang, W. Jiao, Y. Wang, Light olefin synthesis from syngas over sulfide–zeolite composite catalyst, Ind. Eng. Chem. Res 57 (2018) 6815–6820.

[214] Z. Zhang, Y. Huang, H. Ma, W. Qian, H. Zhang, W. Ying, Syngas-to-olefins over MOF-derived ZnZrOx and SAPO-34 bifunctional catalysts, Catal. Commun. 152 (2021) 106292.

[215] L. Tan, F. Wang, P. Zhang, Y. Suzuki, Y. Wu, J. Chen, G. Yang, N. Tsubaki, Design of a core–shell catalyst: an effective strategy for suppressing side reactions in syngas for direct selective conversion to light olefins, Chem. Sci. 11 (2020) 4097–4105.

[216] T. Qiu, L. Wang, S. Lv, B. Sun, Y. Zhang, Z. Liu, W. Yang, J. Li, SAPO-34 zeolite encapsulated Fe3C nanoparticles as highly selective Fischer-Tropsch catalysts for the production of light olefins, Fuel 203 (2017) 811–816.

[217] C. Zhu, M. Zhang, C. Huang, Y. Han, K. Fang, Controlled nanostructure of zeolite crystal encapsulating FeMnK catalysts targeting light olefins from syngas, ACS Appl. Mater. Interfaces 12 (2020) 57950–57962.

[218] D.L.S. Nieskens, A. Ciftci, P.E. Groenendijk, M.F. Wielemaker, A. Malek, Production of light hydrocarbons from syngas using a hybrid catalyst, Ind. Eng. Chem. Res 56 (2017) 2722–2732.

[219] G. Raveendra, C. Li, B. Liu, Y. Cheng, F. Meng, Z. Li, Synthesis of lower olefins from syngas over Zn/Al 2 O 3–SAPO-34 hybrid catalysts: role of doped Zr and influence of the Zn/Al 2 O 3 ratio, Catal. Sci. Technol. 8 (2018) 3527–3538.

[220] G. Raveendra, B. Ma, X. Liu, Y. Guo, Y. Wang, Syngas to light olefin synthesis over La doped Zn x Al y O z composite and SAPO-34 hybrid catalysts, Catal. Sci. Technol. 11 (2021) 3231–3240.